Secondary organic aerosol

1. Atmospheric chemical mechanism for production of molecular constituents

Robert J. Griffin¹

Department of Chemical Engineering, California Institute of Technology, Pasadena, California, USA

Donald Dabdub

Department of Mechanical and Aerospace Engineering, University of California at Irvine, Irvine, California, USA

John H. Seinfeld

Department of Chemical Engineering and Division of Engineering and Applied Science, California Institute of Technology, Pasadena, California, USA

Received 23 February 2001; revised 10 August 2001; accepted 18 December 2001; published 11 September 2002.

[1] This series of three papers addresses the representation of secondary organic aerosol (SOA) in atmospheric models. SOA forms when gas-phase organic species undergo oxidation, leading to products of sufficiently low vapor pressure that can partition between the gas and aerosol phases. The present paper, part 1, is devoted to the development of a gas-phase atmospheric chemical mechanism designed to represent ozone chemistry as well as formation of individual organic oxidation products that are capable of forming SOA. The ozone chemistry in the mechanism draws upon the recent work of Stockwell et al. [1997] and Jenkin et al. [1997] and SAPRC-97 and SAPRC-99 (available from W.P.L. Carter at http://helium.ucr.edu/~carter/). The mechanism is evaluated in the threedimensional California Institute of Technology (CIT) model [Meng et al., 1998] by simulating gas-phase concentrations in the South Coast Air Basin (SoCAB) of California over the period 27-29 August 1987. Total predicted concentrations of gas-phase SOA compounds are compared with levels of SOA that have been inferred on the basis of ambient organic aerosol measurements during this period. These predicted concentrations indicate that the total gas-phase potential of SOA-forming compounds can account for observed aerosol concentrations. Part 2 develops a thermodynamic gas-aerosol partitioning module, and part 3 presents a full three-dimensional simulation of gas and aerosol levels in the SoCAB during a 1993 episode. INDEX TERMS: 0305 Atmospheric Composition and Structure: Aerosols and particles (0345, 4801); 0345 Atmospheric Composition and Structure: Pollution—urban and regional (0305); 0365 Atmospheric Composition and Structure: Troposphere—composition and chemistry; KEYWORDS: secondary organic aerosol, biogenic aerosol, photooxidation, urban air quality

Citation: Griffin, R. J., D. Dabdub, and J. H. Seinfeld, Secondary organic aerosol, 1, Atmospheric chemical mechanism for production of molecular constituents, *J. Geophys. Res.*, 107(D17), 4332, doi:10.1029/2001JD000541, 2002.

1. Introduction

[2] Atmospheric urban and regional scale gas-phase chemical mechanisms describe the formation of oxidants such as ozone (O_3), the hydroxyl radical (OH), and the nitrate radical (NO_3), the consumption of reactive organics, and reactions of the resulting organic peroxy radicals with species such as the oxides of nitrogen ($NO_x = NO + NO_2$). Mech-

Copyright 2002 by the American Geophysical Union. 0148-0227/02/2001JD000541\$09.00

anisms that have been used in urban and regional atmospheric models include that of *Lurmann et al.* [1987] (LCC), the Carbon Bond IV Mechanism (CB-IV) [*Gery et al.*, 1989], the Regional Acid Deposition Model (RADM2) [*Stockwell et al.*, 1990], the Regional Atmospheric Chemistry Model (RACM) [*Stockwell et al.*, 1997], and the Statewide Air Pollution Research Center Mechanism (SAPRC-97) (available from W.P.L. Carter at http://helium. ucr.edu/~carter/) (hereinafter referred to as Carter/SAPRC-97). In addition, *Jenkin et al.* [1997] have presented a master chemical mechanism consisting of 120 parent organic compounds, 2500 chemical species, and approximately 7000 reactions.

[3] Secondary organic aerosol (SOA) is formed in two steps. First, a sufficiently large parent organic is oxidized,

¹Now at Department of Civil and Environmental Engineering, Duke University, Durham, North Carolina, USA.

resulting in products that have vapor pressures significantly lower than that of the parent. If their vapor pressures are low enough, these products can partition to the aerosol phase via condensation (adsorptive or absorptive) or homogeneous nucleation. Because low vapor pressure products are needed to form SOA, in general, only those parent organics with six or more carbon atoms are capable of producing oxidized products that form SOA [Odum et al., 1996]. Existing gasphase atmospheric chemical mechanisms do not include the detailed organic chemistry necessary for prediction of SOA formation. One reason for this is that much of the chemistry of the larger organics that leads to semivolatile products is not known.

[4] This paper describes a new chemical mechanism, termed the Caltech Atmospheric Chemistry Mechanism (CACM), that has two goals: (1) to include state-of-the-art treatment of ozone formation chemistry; and (2) to explicitly predict the concentrations of secondary and tertiary semivolatile oxidation products that have the potential to act as constituents of SOA. In the treatment of O₂ formation chemistry, CACM relies on the recent work of Stockwell et al. [1997], Jenkin et al. [1997], and Carter/SAPRC-97 (see also SAPRC-99 available from W.P.L. Carter at http:// helium.ucr.edu/~carter/) (hereinafter referred to as Carter/ SAPRC-99). The mechanism contains a significant expansion of organic product chemistry in order to predict the formation of multifunctional, low vapor pressure products. In addition to the extension of the mechanism to include more detailed organic chemistry, relevant experimental and empirical information on rate constants and product yields (e.g., alkyl nitrate formation versus NO to NO₂ conversion) have been implemented in CACM [Carter and Atkinson, 1989; Atkinson, 1990, 1994, 1997; Goumri et al., 1992; Lay et al., 1996; Alvarado et al., 1998]. While specific organic chemical mechanisms have been developed to model smog chamber SOA data [see, e.g., Barthelmie and Pryor, 1999], we present here the first detailed atmospheric chemical mechanism that is directed toward explicit prediction of formation of the semivolatile products that could constitute observed SOA. The product distributions in the mechanism to be presented are based either on limited observed product data or on extrapolation of the behavior of smaller organics. We recognize, of course, that precise product specifications are likely to change as more is learned about the mechanisms of SOA formation.

[5] CACM includes a total of 191 species: (1) 120 fully integrated species (fully integrated species have concentrations that are solved for numerically based on kinetics, emission, and deposition) (15 inorganic, 71 reactive organic, and 34 unreactive organic); (2) 67 pseudo-steadystate species (2 inorganic and 65 organic); and (3) 4 species that have fixed concentrations. Table 1 shows a complete list of the species that are included in CACM. Table 2 gives the reactions included in CACM with appropriate Arrhenius rate constant expressions. The goals of the present paper (part 1) are twofold: (1) to describe the inorganic and organic chemistry in the mechanism and (2) to evaluate the performance of the mechanism in simulating gas-phase chemistry during a well-studied episode in the South Coast Air Basin (SoCAB) of California, 27-29 August 1987. Parts 2 and 3, respectively, will derive a module to predict SOA formation based on thermodynamic equilibrium and

present complete gas- and aerosol-phase simulations in the SoCAB for a 1993 episode.

Inorganic Chemistry

[6] Inorganic chemistry within CACM (Reactions 1–42) in Table 2) is derived primarily from the SAPRC-99 mechanism of Carter/SAPRC-99. Only a brief overview of the inorganic chemistry need be given here. Photolysis rate constants are given in Table 3, and rate constants determined by three-body kinetics are listed in Table 4. Additional rate constants not falling into one of these categories are shown in Table 5.

[7] Tropospheric inorganic chemistry is driven by a few relatively well understood reactions. NO is converted to NO_2 primarily via the reaction of NO with O_3 or the peroxy radicals (RO₂ or HO₂) that are formed by the reaction of OH with a number of species. (Reactions of organic species with O₃ or NO₃ also lead to RO₂ formation.) Photolysis of NO₂ results in the formation of $O(^{3}P)$, which combines with O_{2} to form O₃. Photolysis of O₃ leads to formation of both O(³P) and O(¹D), the latter of which reacts with water to form OH. O(¹D) can also be collisionally stabilized to form O(³P). Other reactions that produce OH are the photolysis of HONO, the reaction between O₃ and HO₂, and the photolysis of H₂O₂. HONO is formed by the reactions of OH with NO and NO₂ with H₂O, and H₂O₂ is formed by the selfcombination of HO₂.

[8] The nitrate radical, NO₃, is formed primarily by the combination of NO₂ and O₃ but is relatively unimportant during the day because of its high rate of photolysis. Other sources of NO₃ include the reaction of NO₂ with O(³P) and the oxidation of HNO₃ by OH. HNO₃ is formed in the reaction of NO2 with OH, by the combination of HO2 and NO_3 , or by the hydrolysis of N_2O_5 . (The kinetics of the NO₂-OH reaction [Dransfield et al., 1999] have been significantly updated as compared with those in the extended LCC mechanism used by *Harley et al.* [1993].) HNO₄ is formed by the reaction of NO₂ with HO₂. Sinks for HNO₄ include decomposition and reaction with OH. Oxidation of SO₂ by OH forms SO₃, which is rapidly hydrolyzed to form sulfuric acid (H₂SO₄).

Organic Chemistry

[9] In existing gas-phase urban and regional atmospheric mechanisms, organic chemistry has been focused primarily on predicting the concentrations of peroxy radicals that are generated as a result of hydrocarbon oxidation. In an effort to address the computational demands of gas-phase mechanisms to be used in three-dimensional atmospheric models, parent organics are often lumped into surrogate groups. In CACM, primary organic compounds are lumped in a manner similar to that described by Stockwell et al. [1997]. The result is a set of surrogate compounds designed to represent the entire array of gas-phase organic species emitted to the atmosphere. Oxidation reactions of the surrogate parents are tracked individually, with multiple pathways being represented by the dominant reaction [Kwok and Atkinson, 1995; Atkinson, 1997]. Reactions of the resulting alkyl peroxy radicals are also included. From the reactions of these alkyl peroxy radicals, it is possible to

Table 1. Chemical Species Represented in CACM

Table 1.	1. Chemical Species Represented in CACM			
Term	Description			
	Inorganic, Fully Integrated Species			
NO	nitric oxide			
NO_2	nitrogen dioxide			
O_3	ozone nitrous acid			
HONO HNO ₃	nitric acid			
HNO ₄	pernitric acid			
N_2O_5	nitrogen pentoxide			
NO_3	nitrate radical			
HO_2	hydroperoxy radical			
CO	carbon monoxide			
CO_2 H_2O_2	carbon dioxide hydrogen peroxide			
SO_2	sulfur dioxide			
SO_3	sulfur trioxide			
OH	hydroxyl radical			
	Reactive, Fully Integrated Parent Organic Species			
ETHE	ethene			
OLEL	lumped alkenes C ₃ -C ₆ ^a (1-pentene)			
OLEH	lumped alkenes $> C_6$ (4-methyl-1-octene)			
ALKL	lumped alkanes C_2 - C_6 ^a (2-methyl-butane)			
ALKM ALKH	lumped alkanes C_7 - C_{12}^a (3,5-dimethyl-heptane) lumped alkanes $>$ C ₁₂ (n -hexadecane)			
AROH	lumped aikanes $> C_{12}$ (<i>n</i> -nexadecane) lumped high SOA yield aromatic species (3- <i>n</i> -propyl-toluene)			
AROL	lumped low SOA yield aromatic species (1,2,3-trimethyl-benzene)			
AROO	lumped phenolic species ^a (2,6-dimethyl-phenol)			
ARAL	lumped aromatic monoaldehydes ^a (p-tolualdehyde)			
ARAC ⁺	lumped aromatic monoacids ^a (p-toluic acid)			
PAH	lumped gas-phase polycyclic aromatic hydrocarbons (1,2-dimethyl-naphthalene)			
НСНО	formaldehyde ^a			
ALD2	lumped higher aldehydes ^a (<i>n</i> -pentanal)			
KETL	lumped ketones C_3 - C_6^a (2-pentanone)			
KETH	lumped ketones $> C_6$ (2-heptanone)			
MEOH	methanol			
ETOH ALCH	ethanol lumped higher alcohols (2-hexanol)			
ISOP	isoprene			
BIOL	lumped low SOA yield monoterpene species (α-terpineol)			
BIOH	lumped high SOA yield monoterpene species (γ-terpinene)			
MTBE	methyl-tert-butyl ether			
	Nonreacting, Fully Integrated Organic Species			
$ADAC^{+}$	lumped aromatic diacids (terephthalic acid)			
ACID	lumped organic acids < C ₆			
UR1	3-methyl-heptanoic acid			
UR2 ⁺ UR3 ⁺	3-hydroxy-4-methyl-benzoic acid 2-hydroxy-3-isopropyl-6-keto-heptanoic acid			
UR4	2-isopropyl-5-keto-hexanal			
UR5 ⁺	1-methyl-3-hydroxy-4-isopropyl-1, 2-cyclohexane epoxide			
UR6 ⁺	2-hydroxy-3-isopropyl-6-methyl-cyclohexanone			
UR7 ⁺	3, 7-dimethyl-6-keto-3-octenal			
UR8 ⁺	3-isopropyl-6-keto-3-heptenoic acid			
UR9 UR10	1-methyl-4-isopropyl-1, 2-cyclo-4-hexene epoxide 3-isopropyl-6-methyl-3-cyclohexenone			
UR11 ⁺	1, 2-dimethyl-3-hydroxy-naphthalene			
UR12	1, 2, 3-trimethyl-5-nitro-benzene			
UR13	3- <i>n</i> -propyl-4-nitro-toluene			
UR14 ⁺	2-nitro-4-methyl-benzoic acid			
UR15 ⁺	1, 2-dimethyl-3-nitro-naphthalene			
UR16 UR17 ⁺	2-methyl-2-hydroxy-5-heptanone 2-hydroxy-3-isopropyl-hexadial			
UR18	2-nydroxy-3-isopropyl-nexadiai 3-isopropyl-2-pentendial			
UR19 ⁺	1-methyl-2-formyl-naphthalene			
UR20 ⁺	11-hydroxy-8-hexadecanone			
UR21 ⁺	keto-propanoic acid			
UR22 ⁺	2,6-dimethyl-3,4-dinitro-phenol			
UR23 ⁺ UR24	3-isopropyl-4-hydroxy-2-butenoic acid maleic anhydride			
UR25	maieic annydride 3H-furan-2-one			
UR26 ⁺	4, 5-dimethyl-6-keto-2, 4-heptadienoic acid			
UR27 ⁺	2-carboxy-acetophenone			

UR28 ⁺ UR29 ⁺ UR30 ⁺ UR31 ⁺ UR32 UR33 UR34 ⁺ PAN1 PAN2 PAN3 PAN4 PAN5 PAN6 PAN7 PAN8 ⁺ PAN9 PN10 MGLY	oxalic acid 4-hydroxy-3, 5-dimethyl-2, 4-hexadiendioic acid 2-methyl-5-carboxy-2, 4-hexadiendioic acid 2-(dimethyl-propenoic acid)-benzoic acid 3-methyl-4-heptanone 2-isopropyl-5-keto-2-hexenal 8-hexadecanone **tegrated Secondary Organic Species** peroxy pentionyl nitrate peroxy acetyl nitrate (PAN) unsaturated peroxy propionyl nitrate (PPN) keto-PPN methylene-PPN peroxy nitrate derived from glyoxal peroxy 3-methyl-heptionyl nitrate peroxy 2-hydroxy-3-isopropyl-6-keto-heptionyl nitrate peroxy 3-isopropyl-4-hydroxy-2-butenionyl nitrate
UR30 ⁺ UR31 ⁺ UR32 UR33 UR34 ⁺ PAN1 PAN2 PAN3 PAN4 PAN5 PAN6 PAN7 PAN8 ⁺ PAN9 PN10	2-methyl-5-carboxy-2, 4-hexadiendioic acid 2-(dimethyl-propenoic acid)-benzoic acid 3-methyl-4-heptanone 2-isopropyl-5-keto-2-hexenal 8-hexadecanone ntegrated Secondary Organic Species peroxy pentionyl nitrate peroxy acetyl nitrate (PAN) unsaturated peroxy propionyl nitrate (PPN) keto-PPN methylene-PPN peroxy nitrate derived from glyoxal peroxy 3-methyl-heptionyl nitrate peroxy 2-hydroxy-3-isopropyl-6-keto-heptionyl nitrate
UR31 ⁺ UR32 UR33 UR34 ⁺ PAN1 PAN2 PAN3 PAN4 PAN5 PAN6 PAN7 PAN8 ⁺ PAN9 PN10	2-methyl-5-carboxy-2, 4-hexadiendioic acid 2-(dimethyl-propenoic acid)-benzoic acid 3-methyl-4-heptanone 2-isopropyl-5-keto-2-hexenal 8-hexadecanone ntegrated Secondary Organic Species peroxy pentionyl nitrate peroxy acetyl nitrate (PAN) unsaturated peroxy propionyl nitrate (PPN) keto-PPN methylene-PPN peroxy nitrate derived from glyoxal peroxy 3-methyl-heptionyl nitrate peroxy 2-hydroxy-3-isopropyl-6-keto-heptionyl nitrate
UR32 UR33 UR34 ⁺ Reactive, Fully In PAN1 PAN2 PAN3 PAN4 PAN5 PAN6 PAN7 PAN8 ⁺ PAN9 PN10	3-methyl-4-heptanone 2-isopropyl-5-keto-2-hexenal 8-hexadecanone **mtegrated Secondary Organic Species** peroxy pentionyl nitrate peroxy acetyl nitrate (PAN) unsaturated peroxy propionyl nitrate (PPN) keto-PPN methylene-PPN peroxy nitrate derived from glyoxal peroxy 3-methyl-heptionyl nitrate peroxy 2-hydroxy-3-isopropyl-6-keto-heptionyl nitrate
UR33 UR34 ⁺ Reactive, Fully In PAN1 PAN2 PAN3 PAN4 PAN5 PAN6 PAN7 PAN8 ⁺ PAN9 PN10	3-methyl-4-heptanone 2-isopropyl-5-keto-2-hexenal 8-hexadecanone **mtegrated Secondary Organic Species** peroxy pentionyl nitrate peroxy acetyl nitrate (PAN) unsaturated peroxy propionyl nitrate (PPN) keto-PPN methylene-PPN peroxy nitrate derived from glyoxal peroxy 3-methyl-heptionyl nitrate peroxy 2-hydroxy-3-isopropyl-6-keto-heptionyl nitrate
UR34 ⁺ Reactive, Fully In PAN1 PAN2 PAN3 PAN4 PAN5 PAN6 PAN7 PAN8 ⁺ PAN9 PN10	8-hexadecanone ntegrated Secondary Organic Species peroxy pentionyl nitrate peroxy acetyl nitrate (PAN) unsaturated peroxy propionyl nitrate (PPN) keto-PPN methylene-PPN peroxy nitrate derived from glyoxal peroxy 3-methyl-heptionyl nitrate peroxy 2-hydroxy-3-isopropyl-6-keto-heptionyl nitrate
Reactive, Fully In PAN1 PAN2 PAN3 PAN4 PAN5 PAN6 PAN7 PAN8 ⁺ PAN9 PN10	peroxy pentionyl nitrate peroxy acetyl nitrate (PAN) unsaturated peroxy propionyl nitrate (PPN) keto-PPN methylene-PPN peroxy nitrate derived from glyoxal peroxy 3-methyl-heptionyl nitrate peroxy 2-hydroxy-3-isopropyl-6-keto-heptionyl nitrate
PAN1 PAN2 PAN3 PAN4 PAN5 PAN6 PAN7 PAN8 ⁺ PAN9 PN10	peroxy pentionyl nitrate peroxy acetyl nitrate (PAN) unsaturated peroxy propionyl nitrate (PPN) keto-PPN methylene-PPN peroxy nitrate derived from glyoxal peroxy 3-methyl-heptionyl nitrate peroxy 2-hydroxy-3-isopropyl-6-keto-heptionyl nitrate
PAN1 PAN2 PAN3 PAN4 PAN5 PAN6 PAN7 PAN8 ⁺ PAN9	peroxy pentionyl nitrate peroxy acetyl nitrate (PAN) unsaturated peroxy propionyl nitrate (PPN) keto-PPN methylene-PPN peroxy nitrate derived from glyoxal peroxy 3-methyl-heptionyl nitrate peroxy 2-hydroxy-3-isopropyl-6-keto-heptionyl nitrate
PAN3 PAN4 PAN5 PAN6 PAN7 PAN8 ⁺ PAN9 PN10	unsaturated peroxy propionyl nitrate (PPN) keto-PPN methylene-PPN peroxy nitrate derived from glyoxal peroxy 3-methyl-heptionyl nitrate peroxy 2-hydroxy-3-isopropyl-6-keto-heptionyl nitrate
PAN4 PAN5 PAN6 PAN7 PAN8 ⁺ PAN9 PN10	keto-PPN methylene-PPN peroxy nitrate derived from glyoxal peroxy 3-methyl-heptionyl nitrate peroxy 2-hydroxy-3-isopropyl-6-keto-heptionyl nitrate
PAN5 PAN6 PAN7 PAN8 ⁺ PAN9 PN10	methylene-PPN peroxy nitrate derived from glyoxal peroxy 3-methyl-heptionyl nitrate peroxy 2-hydroxy-3-isopropyl-6-keto-heptionyl nitrate
PAN6 PAN7 PAN8 ⁺ PAN9 PN10	peroxy nitrate derived from glyoxal peroxy 3-methyl-heptionyl nitrate peroxy 2-hydroxy-3-isopropyl-6-keto-heptionyl nitrate
PAN7 PAN8 ⁺ PAN9 PN10	peroxy 3-methyl-heptionyl nitrate peroxy 2-hydroxy-3-isopropyl-6-keto-heptionyl nitrate
PAN8 ⁺ PAN9 PN10	peroxy 2-hydroxy-3-isopropyl-6-keto-heptionyl nitrate
PAN9 PN10	
PN10	peroxy 3-isopropyl-4-nydroxy-2-butenionyl nitrate
MGLI	peroxy nitrate derived from glyoxalic acid methyl glyoxal
MVK	methyl-vinyl-ketone
MCR	methacrolein
RPR1	3-methyl-heptanal
RPR2	3-hydroxy-4-methyl-benzaldehyde
RPR3 ⁺	2-hydroxy-3-isopropyl-6-keto-heptanal
RPR4 ⁺	2,6-dimethyl-4-nitro-phenol
RPR5	2-nitro-4-methyl-benzaldehyde
RPR6	benzene-1, 4-dialdehyde
RPR7 ⁺	4-formyl-benzoic acid
RPR8	3-isopropyl-4-hydroxy-2-butenal
RPR9 ⁺	4-hydroxy-3, 5-dimethyl-2, 4-hexadiendial
RP10	2-methyl-butenalic acid
RP11	4, 5-dimethyl-6-keto-2, 4-heptadienal
RP12 ⁺	2-methyl-5-formyl-2, 4-hexadiendial
RP13 ⁺	2-carboxyl-5-methyl-2, 4-hexadiendial
RP14 ⁺ RP15	2-(dimethyl-propenal)-benzaldehyde 2-formyl-acetophenone
RP16	glyoxalic acid
RP17 ⁺	4-hydroxy-3, 5-dimethyl-2, 4-hexadienalic acid
RP18 ⁺	2-methyl-5-formyl-2, 4-hexadiendioic acid
RP19 ⁺	2-(dimethyl-propenal)-benzoic acid
AP1 ⁺	2-nitrooxymethyl-6-methyl-phenol
AP2	2-methyl-2-hydroxy-5-heptylnitrate
AP3	3-methyl-4-heptylnitrate
AP4	1, 2-dimethyl-3-nitrooxymethyl-benzene
AP5	4-nitrooxymethyl-benzaldehyde
$AP6^+$	4-nitrooxymethyl-benzoic acid
AP7	1-methyl-1-nitrato-2, 3-dihydroxy-4-isopropyl-cyclohexane
AP8 ⁺	1-methyl-4-nitrato-4-isopropyl-5-hydroxy-cyclohexene
AP9	5-isopropyl-6-nitrato-4-hexen-2-one
AP10 ⁺	1-methyl-2-nitrooxymethyl-naphthalene
AP11 ⁺ AP12 ⁺	8-hexadecylnitrate
RO ₂ T	8-hydroxy-11-hexadecylnitrate total organic peroxy radical
RO ₂ 1 RO ₂ 8	acetyl peroxy radical
OSD Reactive, Inorg	ganic Pseudo-Steady State Species O (¹ D)
0	O (³ P)
Donativa Our	anic Pseudo-Steady State Species
RO ₂ 1	methyl peroxy radical from oxidation of CH ₄
RO ₂ 1 RO ₂ 2	hydroxy alkyl peroxy radical $< C_6$ from oxidation of ETHE, ETOH,
- <u>-</u>	OLEL, and ALCH (C ₄ , 1-peroxy, 2-hydroxy)
RO_23	nitrato alkyl peroxy radical $< C_6$ from oxidation of ETHE and
-	OLEL (C ₄ , 1-nitrato, 2-peroxy)
RO_24	aldehydic alkyl peroxy radical from oxidation of ISOP and ETHE (C_2)
RO_2^25	alkyl peroxy radical $< C_6$ from oxidation of KETL, ISOP, ALKL,
	BIOH, and OLEL (C ₃ , 1-peroxy)
RO_26	acyl radical from aldehydic H abstraction of ALD2
RO_2^{-7}	keto alkyl peroxy radical $< C_6$ from oxidation of ISOP and KETL
	$(C_4, 2\text{-keto}, 3\text{-peroxy})$

Table 1. (continued)

Term	Description
RO ₂ 9	branched hydroxy alkenyl peroxy radical from oxidation of ISOP
	(C ₄ chain, 1-hydroxy, 2-methyl, 2-peroxy)
RO ₂ 10	branched hydroxy alkenyl peroxy radical from oxidation of ISOP
PO 11	(C ₄ chain, 2-methyl, 3-peroxy, 4-hydroxy)
RO ₂ 11	branched nitrato alkenyl peroxy radical from oxidation of ISOP
RO ₂ 12	(C ₄ chain, 1-nitrato, 2-methyl, 2-peroxy) branched nitrato alkenyl peroxy radical from oxidation of ISOP
10212	(C ₄ chain, 2-methyl, 3-peroxy, 4-nitrato)
RO ₂ 13	keto alkenyl peroxy radical from oxidation of ISOP
PO 14	$(C_4, 3\text{-keto}, 4\text{-peroxy})$
RO ₂ 14	alkenyl peroxy radical from oxidation of ISOP (C ₂)
RO ₂ 15	ether alkyl peroxy radical from oxidation of MTBE (C ₅ , accounts for attack on both sides of the ether bond)
RO ₂ 16	keto alkyl peroxy radical from oxidation of KETH (C_7 , 2-keto,
	3-peroxy)
RO ₂ 17	aromatic peroxy radical from side chain oxidation of AROO
RO ₂ 18	branched hydroxy alkyl peroxy radical $> C_6$ from oxidation of OLEH and ALKM (C_7 chain, 2-methyl, 2-hydroxy, 5-peroxy)
RO ₂ 19	branched nitrato alkyl peroxy radical from oxidation of OLEH
	(C ₈ chain, 4-methyl, 1-nitrato, 2-peroxy)
RO_220	branched alkyl peroxy radical > C ₆ from oxidation of OLEH and
PO 21	ALKM (C ₇ chain, 3-methyl, 4-peroxy)
RO ₂ 21 RO ₂ 22	aromatic peroxy radical from side chain oxidation of AROL aromatic peroxy radical from side chain oxidation of ARAL
RO ₂ 22 RO ₂ 23	aromatic peroxy radical from side chain oxidation of ARAC
RO ₂ 24	cyclic dihydroxy alkyl peroxy radical from OH oxidation of BIOL
	(C ₆ cycle, 1-methyl, 1-peroxy, 2, 3-dihydroxy, 4-isopropyl)
RO_225	cyclic hydroxy nitrato alkyl peroxy radical from NO ₃ oxidation of BIOL
RO ₂ 26	(C_6 cycle, 1-methyl, 1-peroxy, 2-nitrato, 3-hydroxy, 4-isopropyl) branched keto hydroxy aldehydic peroxy radical from oxidation of
KO ₂ 20	BIOL (C ₇ chain, 2-hydroxy, 3-isopropyl, 5-peroxy, 6-keto)
RO ₂ 27	cyclic hydroxy alkenyl peroxy radical from oxidation of BIOH
	(C ₆ cycle, 1-methyl, 1-ene, 4-peroxy, 4-isopropyl, 5-hydroxy)
RO_228	cyclic nitrato alkenyl peroxy radical from oxidation of BIOH
RO ₂ 29	(C ₆ cycle, 1-methyl, 1-ene, 4-peroxy, 4-isopropyl, 5-nitrato) branched keto alkenyl peroxy radical from oxidation of BIOH
KO ₂ 2)	(C ₆ chain, 1-peroxy, 2-isopropyl, 2-ene, 5-keto)
RO ₂ 30	branched keto aldehydic peroxy radical from oxidation of BIOH
	(C ₇ chain, 3-isopropyl, 3-ene, 5-peroxy, 6-keto)
RO ₂ 31	aromatic peroxy radical from side chain oxidation of PAH
RO ₂ 32 RO ₂ 33	alkyl peroxy radical from oxidation of ALKH (8-peroxy) peroxy radical from addition of O_2 to RAD2
RO ₂ 34	peroxy radical from addition of O ₂ to RAD3
RO_2^2 35	peroxy radical from addition of O ₂ to RAD4
RO_236	peroxy radical from addition of O2 to RAD5
RO ₂ 37	peroxy radical from addition of O ₂ to RAD6
RO ₂ 38	peroxy radical from addition of O ₂ to RAD7
RO ₂ 39 RO ₂ 40	unsaturated acyl peroxy radical from oxidation of ISOP (C ₃) branched hydroxy keto alkenyl peroxy radical from oxidation of BIOH
KO240	(C ₆ chain, 1-hydroxy, 2-isopropyl, 2-ene, 4-peroxy, 5-keto)
RO ₂ 41	hydroxy alkyl peroxy radical from oxidation of ALKH (8-hydroxy,
	11-peroxy)
RO ₂ 42	bicyclic peroxy radical from the O ₂ bridging in RO ₂ 33
RO ₂ 43 RO ₂ 44	bicyclic peroxy radical from the O ₂ bridging in RO ₂ 34 bicyclic peroxy radical from the O ₂ bridging in RO ₂ 35
RO ₂ 45	bicyclic peroxy radical from the O ₂ bridging in RO ₂ 36
RO ₂ 46	bicyclic peroxy radical from the O ₂ bridging in RO ₂ 37
RO_2^-47	bicyclic peroxy radical from the O ₂ bridging in RO ₂ 38
RO ₂ 48	acyl radical from aldehydic H abstraction of MGLY
RO ₂ 49	peroxy radical formed from OH oxidation of MVK
RO ₂ 50 RO ₂ 51	acyl radical from aldehydic H abstraction of MCR peroxy radical from OH addition to double bond in MCR
RO ₂ 51 RO ₂ 52	peroxy radical from NO ₃ addition to double bond in MCR
RO ₂ 53	dicarbonyl peroxy radical from MCR/O ₃ reaction (C ₃ chain,
	1-peroxy, 2-keto, 3-aldehydic)
RO ₂ 54	acyl radical from decomposition of RO ₂ 53
RO ₂ 55	acyl radical from aldehydic H abstraction of RPR1
RO ₂ 56 RO ₂ 57	acyl radical from aldehydic H abstraction of RPR3 acyl radical from aldehydic H abstraction of RPR7
RO ₂ 57 RO ₂ 58	acyl acid peroxy radical from aldehydic H abstraction of RP16 (C ₂)
RAD1	radical from NO ₃ oxidation of AROO
RAD2	hexadienyl radical from OH oxidation of AROO
RAD3	hexadienyl radical from OH oxidation of AROL

Table 1. (continued)

Term	Description
RAD4	hexadienyl radical from OH oxidation of AROH
RAD5	hexadienyl radical from OH oxidation of ARAL
RAD6	hexadienyl radical from OH oxidation of ARAC
RAD7	hexadienyl radical from OH oxidation of PAH
RAD8	radical from NO ₃ oxidation of RPR4
	Species With Concentrations Not Affected by Reaction
H_2O	water vapor
O_2	oxygen
M	third body
CH ₄	methane

^a Also formed in CACM.

predict the formation of surrogate oxidation products. If a product is considered reactive, it can go on to form tertiary (and so on) oxidation products. Prediction of specific products is important because gas-particle partitioning, through the link to vapor pressure, is highly dependent on molecular size and degree of functionality [Yu et al., 1999; Pankow et al., 2001]. Concentrations of the secondary, tertiary, etc., oxidation products then allow for prediction of the partitioning of organic molecules between the gasand aerosol phases (part 2).

[10] In CACM, the lumped model compound corresponding to a given individual parent hydrocarbon is determined by considering the size of the molecule, its structural characteristics (e.g., branched versus cyclic versus straight chain), its functionality (both location and type), its reactivity, and its experimentally determined potential for forming SOA, if available. Taking the "average" structure of the compounds within a group (a group being appropriately defined) yields the surrogate for each group. Twenty-three individual groups, either surrogates or those described explicitly, are used (see Table 1). Instead of generating an aggregate rate constant for the surrogates as described by Stockwell et al. [1997], the rate constant for the model parent is used (either based on experimental data or calculated using structure-reactivity relationships; see Tables 2 and 6).

3.1. Alkanes

[11] Alkanes are found in significant quantity in urban atmospheres [Fraser et al., 1997; Schauer, 1998; Schauer et al., 1999a, 1999b]. Methane chemistry is included explicitly in CACM, but because of its large mixing ratio, the concentration of methane remains fixed. The main tropospheric loss process for methane is the well-documented oxidation by OH (reaction 43) to form the methyl peroxy radical (RO₂1). RO₂1 can then react with NO (reaction 110) in the presence of O_2 to form HO_2 , formaldehyde (HCHO), and NO₂, with other peroxy radicals (represented henceforth as RO₂T) (reaction 111) to yield HCHO and HO₂, or with HO₂ to form HCHO (reaction 112). Throughout CACM, alkyl peroxy radical reactions with RO2T are assumed, for simplicity, to form the same products as the NO reaction that results in the conversion of NO to NO₂. In addition, reactions with HO₂ are assumed to form the degradation products of the corresponding intermediate hydroperoxide

since hydroperoxides are relatively reactive and often form very similar products upon oxidation [Seinfeld and Pandis, 1998]. To account accurately for RO_2T (which is formed along with every individual RO_2i species) concentrations, its reactions with NO, HO_2 , and itself are also included in CACM (reactions 94–96).

3.1.1. Short Chain Alkanes

[12] Short chain alkanes (ALKL) are considered as those with two to six carbon atoms. Based on the structural aggregation, 2-methyl-butane is used to represent these compounds, as shown in Table 1. In general, alkanes with more than one carbon atom are oxidized by OH abstraction of an H-atom with the subsequent addition of O_2 to form the alkyl peroxy radical [Atkinson, 1997]. As discussed above, the alkyl peroxy radical further reacts with NO, HO₂, or RO₂T. In the case of ALKL, oxidation by OH (reaction 58) results in the formation of RO₂5, which is a lumped alkyl peroxy radical formed by other parent hydrocarbons as well. RO₂5 is treated as a primary peroxy radical with three carbon atoms and upon reaction with NO (reaction 122), can form the corresponding alkyl nitrate or NO2, HO2, and the corresponding aldehyde. The yield of alkyl nitrate formation versus NO to NO2 conversion is calculated based on Carter and Atkinson [1989]. The HO₂ and RO₂T reactions also form HO₂ and an aldehyde (ALD2) (reactions 123 and 124). In this case, the alkyl nitrate formed in the NO reaction is treated as ALKL. When reactive small chain compounds that are not expected to contribute to SOA (either by dissolving in an aqueous phase or by absorption into an organic phase) are formed, they are reclassified within parent groups according to their size and most reactive functional group.

3.1.2. Medium Chain Alkanes

[13] Medium chain alkanes (ALKM) are taken as those with 7 to 12 carbon atoms and are represented by 3,5-dimethyl-heptane. Initial OH oxidation of this species forms RO₂20 (reaction 78). Like the corresponding RO₂5, RO₂20 is formed by more than one parent species and is represented by a lumped structure, 3-methyl-4-heptyl-peroxy radical. RO₂20 reacts similarly to RO₂5 (reactions 176–178) including the formation of an alkyl nitrate (AP3). (Alkyl nitrates with the potential to partition to the aerosol phase are labeled as APi.) The alkoxy radical formed in these reactions, however, has sufficient chain length that the dominant mechanism involving this radical proceeds by isomerization through a 1,5-H shift [Atkinson, 1997]. The

Table 2. Reactions Contained in the Caltech Atmospheric Chemistry Mechanism

Reaction	Reactants	Products	Rate Constants, ^a cm molecule ⁻¹ s ⁻¹	References, Comments
1	$NO_2 + hv$	NO + O	see Table 3	1
2	$O + O_2 + M$	$O_3 + M$	$5.53E + 16/TEMP^4.8$	2
3	$O + NO_2$	$NO + O_2$	$6.5E-12 \times EXP(119.8/TEMP)$	2
4	$O + NO_2 + M$	$NO_3 + M$	see Table 4	2
5	$NO + O_3$	$NO_2 + O_2$	$1.8E-12 \times EXP(-1368.9/TEMP)$	2
6	$NO_2 + O_3$	$NO_3 + O_2$	$1.4E-13 \times EXP(-2471.1/TEMP)$	2
7	$NO + NO_3$	2 NO ₂	$1.8\text{E-}11 \times \text{EXP}(110.7/\text{TEMP})$	2 2
8	$NO + NO + O_2$	2 NO ₂	$5.09\text{E}-18/\text{TEMP} \times \text{EXP}(528.4/\text{TEMP})$	
9	$NO_2 + NO_3 + M$	$N_2O_5 + M$	see Table 4	2 2
10	N_2O_5	$NO_2 + NO_3$	see Table 4	2 2
11 12	$N_2O_5 + H_2O$	2 HNO_3	2.59E-22 4.5E-14 × EXP(-1258.2/TEMP)	2
	$NO_2 + NO_3$	$NO + NO_2 + O_2$	` ,	1
13 14	$NO_3 + hv$ $NO_3 + hv$	$NO + O_2$	see Table 3 see Table 3	1
15	$O_3 + hv$	$NO_2 + O$ $O + O_2$	see Table 3	1
16	$O_3 + hv$ $O_3 + hv$	$OSD + O_2$	see Table 3	1
17	$OSD + H_2O$	2 OH	2.2E-10	2
18	$OSD + II_2O$ OSD + M	O + M	$1.53E + 11/TEMP \times EXP(95.6/TEMP)$	2
19	NO + OH + M	HONO + M	see Table 4 $\times EAF(93.0/1EMF)$	2
20	HONO + hv	$0.9 \text{ NO} + 0.1 \text{ NO}_2 + 0.9 \text{ OH}$	see Table 3	1
20	HONO $\pm nv$	+ 0.1 HO ₂	see Table 3	1
21	$NO_2 + H_2O$	$HONO - NO_2 + HNO_3$	4.0E-24	1
22	$NO_2 + OH + M$	$HNO_3 + M$	see Table 4	3
23	$HNO_3 + OH$	$NO_3 + H_2O$	see Table 5	2
24	CO + OH	$HO_2 + CO_2$	see Table 5	2
25	$O_3 + OH$	$HO_2 + O_2$ $HO_2 + O_2$	$1.9E-12 \times EXP(-1001.5/TEMP)$	2
26	$NO + HO_2$	$NO_2 + OH$	$3.41E-12 \times EXP(271.8/TEMP)$	2
27	$NO_2 + HO_2 + M$	$HNO_4 + M$	see Table 4	2
28	HNO ₄	$NO_2 + HO_2$	see Table 4	2
29	$HNO_4 + OH$	$NO_2 + O_2 + H_2O$	$1.5E-12 \times EXP(362.4/TEMP)$	2
30	$O_3 + HO_2$	OH + 2 O2	$1.4E-14 \times EXP(-598.9/TEMP)$	2
31	$HO_2 + HO_2$	H_2O_2	see Table 5	2
32	$HO_2 + HO_2 + H_2O$	$H_2O_2 + O_2 + H_2O$	see Table 5	2
33	$NO_3 + HO_2$	$0.8 \text{ NO}_2 + 0.2 \text{ HNO}_3 + 0.8 \text{ OH} + \text{O}_2$	4.0E-12	2
34	$O + O_3$	2 O ₂	$8.0\text{E-}12 \times \text{EXP}(-2058.4/\text{TEMP})$	2
35	$SO_2 + OH$	H_2SO_4 (via SO_3) + HO_2	see Table 4	2
36	$H_2O_2 + hv$	2 OH	see Table 3	1
37	$H_2O_2 + OH$	$HO_2 + H_2O$	$2.91\text{E-}12 \times \text{EXP}(-161/\text{TEMP})$	1
38	O + NO + M	$NO_2 + M$	6.75E-06/TEMP^2.6	2
39	HONO + OH	$NO_2 + H_2O$	$2.7E-12 \times EXP(261.7/TEMP)$	2 2 2 2
40	$NO_3 + OH$	$NO_2 + HO_2$	2.0E-11	2
41	$NO_3 + NO_3$	$2 \text{ NO}_2 + \text{O}_2$	$8.5E-13 \times EXP(-2450.9/TEMP)$	2
42	$OH + HO_2$	$H_2O + O_2$	$4.8E-11 \times EXP(251.6/TEMP)$	2
43	$CH_4 + OH$	$RO_21 + RO_2T + H_2O$	$2.66E-12 \times EXP(-1800.2/TEMP)$	2
44	HCHO + hv	$CO + 2 HO_2$	see Table 3	1
45	HCHO + hv	$CO + H_2$	see Table 3	1
46	HCHO + OH	$CO + HO_2 + H_2O$	$1.2E-14 \times TEMP \times EXP(286.9/TEMP)$	4
47	HCHO + NO ₃	$HNO_3 + CO + HO_2$	$2.0E-12 \times EXP(-2430.8/TEMP)$	2 4
48	MEOH + OH	$HO_2 + HCHO + H_2O$	6.0E-18 × TEMP^2 × EXP(170.1/TEMP)	
49 50	ETHE + OH	$RO_22 + RO_2T$ $RO_23 + RO_2T$	$1.96E-12 \times EXP(437.8/TEMP)$ $4.89E-18 \times TEMP^2 \times EXP(-2282.3/TEMP)$	5 5
51	$ETHE + NO_3$ $ETHE + O_3$	0.315 CO + 0.06 HO ₂ + 0.06 OH + 0.185 ACID + 0.5 HCHO + 0.07 H ₂ O	9.14E-15 × EXP(-2580.3/TEMP)	5
52	ETHE + O	$0.6 \text{ CO} + \text{HO}_2 + 0.6 \text{ RO}_2 \text{1} + 0.4 \text{ RO}_2 \text{4} + \text{RO}_2 \text{T}$	7.3E-13	5
53	ETOH + OH	CF(1) HO ₂ + CF(1) ALD2 + CF(2) RO ₂ 2 + CF(2) RO ₂ T + H ₂ O	$6.18E-18 \times TEMP^2 \times EXP(532/TEMP)$	4
54	OLEL + OH	$RO_2 2 + RO_2 T$	$5.86E-12 \times EXP(500.3/TEMP)$	4
55	$OLEL + NO_3$	$RO_2^23 + RO_2^2T$	$1.0\text{E}-13 \times \text{EXP}(-800.2/\text{TEMP})$	5
56	OLEL + O ₃	0.56 CO + 0.2 CO ₂ + 0.36 OH + 0.28 HO ₂ + 0.5 HCHO + 0.5 ALD2 + 0.24 ACID + 0.1 ALKL + 0.28 RO ₂ 5 + 0.28 RO ₋ T	1.0E-17	5
57	OLEL + O	+ 0.28 RO ₂ T 0.5 ALKL + 0.4 ALD2 + 0.1 RO ₂ 4 + 0.1 RO ₂ 5 + 0.2 RO ₂ T	4.66E-12	5
58	ALKL + OH	$RO_2 + RO_2 + H_2O$	3.91E-12	4
59	ALD2 + hv	$CO + HO_2 + RO_2 + RO_2 T$	see Table 3	i
-	**	2 - 22-		

Table 2. (continued)

Table 2.	(continued)			
Reaction	Reactants	Products	Rate Constants, a cm molecule 1 s -1	References, Comments
60	ALD2 + OH	$RO_26 + RO_2T + H_2O$	6.91E-12 × EXP(250/TEMP)	1
61	$ALD2 + NO_3$	$HNO_3 + RO_26 + RO_2T$	$3.0\text{E-}13 \times \text{EXP}(-1427/\text{TEMP})$	1
62	KETL + OH	$RO_27 + RO_2T + H_2O$	4.91E-12	6
63	KETL + hv	$RO_25 + RO_28 + 2 RO_2T$	see Table 3	1
64	ISOP + OH	$0.66 \text{ RO}_29 + 0.34 \text{ RO}_210 + \text{RO}_2T$	2.55E-11 × EXP(410.2/TEMP)	5
65 66	$ISOP + NO_3$ $ISOP + O_3$	$0.66 \text{ RO}_211 + 0.34 \text{ RO}_212 + \text{RO}_2\text{T}$	$3.02E-12 \times EXP(-445.9/TEMP)$	5 5
00	ISOP + O ₃	0.068 CO ₂ + 0.461 CO + 0.5 HCHO + 0.664 OH + 0.366 HO ₂ + 0.054 OLEL + 0.121 ACID + 0.389 MVK + 0.17 MCR + 0.271 RO ₂ 13 + 0.095 RO ₂ 14 + 0.366 RO ₂ T	7.86E-15 × EXP(-1912.9/TEMP)	3
67	ISOP + O	0.925 OLEL + 0.075 ALD2	3.5E-11	5
68	MTBE + OH	$RO_215 + RO_2T + H_2O$	3.2E-12	7
69	ALCH + OH	$RO_22 + RO_2T + H_2O$	see Table 6	8
70	KETH + OH	$RO_216 + RO_2T + H_2O$	see Table 6	8
71	KETH + hv	$RO_25 + RO_28 + 2 RO_2T$	see Table 3	1
72	$AROO + NO_3$	$HNO_3 + RAD1$	3.77E-12	2
73	AROO + OH	0.16 HO ₂ + 0.16 AROO + 0.1 RO ₂ 17 + 0.1 RO ₂ T + 0.74 RAD2 + 0.1 H ₂ O	see Table 6	8
74	OLEH + OH	$RO_218 + RO_2T$	see Table 6	8
75	$OLEH + NO_3$	$RO_2^219 + RO_2^2T$	$k_{74} \times k_{55}/k_{54}$	estimated k
76	OLEH + O ₃	0.56 CO + 0.2 CO ₂ + 0.36 OH + 0.28 HO ₂ + 0.5 HCHO + 0.5 RPR1 + 0.12 ACID + 0.12 UR1 + 0.1 ALKM + 0.28 RO ₂ 20 + 0.28 RO ₂ T	$k_{74} \times k_{56}/k_{54}$	estimated k
77	OLEH + O	0.5 ALKM + 0.4 RPR1 + 0.1 RO ₂ 4 + 0.1 RO ₂ 20 + 0.2 RO ₂ T	$k_{74}k \times {}_{57}/k_{54}$	estimated k
78	ALKM + OH	$RO_220 + RO_2T + H_2O$	see Table 6	8
79	AROL + OH	0.16 HO ₂ + 0.16 AROO + 0.06 RO ₂ 21 + 0.78 RAD3 + 0.06 RO ₂ T+ 0.06 H ₂ O	3.27E-11	4
80	AROH + OH	0.16 HO ₂ + 0.16 AROO + 0.84 RAD4	see Table 6	8
81 82	ARAL + NO ₃ ARAL + OH	HNO ₃ + O ₃ - HO ₂ + ARAC 0.16 RPR2 + (0.16-CF(39)) HO ₂ + CF(39) O ₃ + CF(39) ARAC + CF(45) RO ₂ 22 + CF(40) RAD5 + CF(45) RO ₂ T + (CF(39) + CF(45))H ₂ O	1.4E-12 × EXP(-1872.2/TEMP) 1.29E-11	2 2
83	ARAC + OH	0.16 HO ₂ + 0.16 UR2 + 0.1 RO ₂ 23 + 0.74 RAD6 + 0.1 RO ₂ T + 0.1 H ₂ O	see Table 6	8
84	BIOL + OH	$RO_224 + RO_2T$	1.7E-10	9
85	BIOL + NO ₃	$RO_225 + RO_2T$	1.46E-11	9
86	$BIOL + O_3$	0.445 CO + 0.055 H ₂ O ₂ + 0.445 HO ₂ + 0.89 OH + 0.055 UR3 + 0.445 UR4 + 0.055 RPR3 + 0.445 RO ₂ 26 + 0.445 RO ₂ T	2.5E-16	9
87	BIOL + O	0.75 UR5 + 0.25 UR6	$k_{84} \times k_{57}/k_{54}$	estimated k
88	BIOH + OH	$RO_227 + RO_2T$	1.77E-10	5
89	$BIOH + NO_3$	$RO_228 + RO_2T$	2.91E-11	5
90	$BIOH + O_3$	0.445 CO + 0.055 H ₂ O ₂ + 0.89 OH + 0.055 UR7 + 0.055 UR8 + 0.445 RO ₂ 29 + 0.445 RO ₂ 30 + 0.89 RO ₂ T	1.4E-16	5
91 92	BIOH + O PAH + OH	0.75 UR9 + 0.25 UR10 0.16 HO ₂ + 0.16 UR11 + 0.1 RO ₂ 31 + 0.74 RAD7 + 0.1 RO ₂ T + 0.1 H ₂ O	8.59E-11 7.7E-11	5 6
93	ALKH + OH	$RO_232 + RO_2T + H_2O$	see Table 6	8
94	$RO_2T + HO_2$	HO_2	3.41E-13 \times EXP(800.2/TEMP)	2
95	$RO_2T + NO$	NO NO	$4.2E-12 \times EXP(181.2/TEMP)$	2
96	$RO_2T + RO_2T$	RO_2T	1.0E-15	2
97	$RAD2 + O_2$	$RO_233 + RO_2T$	7.7E + 5/TEMP	10
98	$RAD3 + O_2$	$RO_234 + RO_2T$	k ₉₇	
99	$RAD4 + O_2$	$RO_235 + RO_2T$	k_{97}	

Table 2. (continued)

Table 2.	(continuea)			
Reaction	Reactants	Products	Rate Constants, a cm molecule 1 s -1	References, Comments
100	$RAD5 + O_2$	$RO_236 + RO_2T$	k ₉₇	
101	$RAD6 + O_2$	$RO_2SO + RO_2T$ $RO_2SO + RO_2T$	k ₉₇	
102	$RAD7 + O_2$	$RO_238 + RO_2T$	k ₉₇	
103	$RAD1 + NO_2$	RPR4	3.0E-11	10
104	$RAD2 + NO_2$	$RPR4 + H_2O$	k_{103}	
105	$RAD3 + NO_2$	$UR12 + H_2O$	k_{103}	
106	$RAD4 + NO_2$	$UR13 + H_2O$	k_{103}	
107 108	$RAD5 + NO_2$ RAD6 + NO	$RPR5 + H_2O$ $LIP14 + H_2O$	k_{103}	
109	$RAD6 + NO_2$ $RAD7 + NO_2$	$UR14 + H_2O$ $UR15 + H_2O$	$rac{k_{103}}{k_{103}}$	
110	$RO_21 + NO$	$NO_2 + HO_2 + HCHO$	$4.09E-12 \times EXP(180.2/TEMP)$	11
111	$RO_21 + RO_2T$	$HO_2 + HCHO + RO_2T + O_2$	k ₉₆	
112	$RO_2^21 + HO_2$	$HO_2 + OH + HCHO$	k_{94}	
113	$RO_22 + NO$	$NO_2 + HO_2 + HCHO + ALD2$	$2.45E-12 \times EXP(180.2/TEMP)$	11
114	$RO_22 + RO_2T$	$HO_2 + HCHO + ALD2 + RO_2T + O_2$	k_{96}	
115	$RO_22 + HO_2$	$OH + HO_2 + HCHO + ALD2$	k_{94}	
116	$RO_23 + NO$	$2 \text{ NO}_2 + \text{HCHO} + \text{ALD2}$	k_{113}	
117	$RO_23 + RO_2T$	$NO_2 + HO_2 + HCHO + ALD2$ + $O_2 + RO_2T$	k ₉₆	
118	$RO_23 + HO_2$	$NO_2 + HO_2 + OH + HCHO + ALD2$	k_{94}	
119	$RO_24 + NO$	$NO_2 + CO + HO_2 + HCHO$	$3.45E-12 \times EXP(180.2/TEMP)$	11
120	$RO_24 + RO_2T$	$CO + HO_2 + HCHO + RO_2T + O_2$	k ₉₆	
121	$RO_24 + HO_2$	$CO + HO_2 + OH + HCHO$	k_{94}	
122	$RO_25 + NO$	$CF(3)$ ALKL + $CF(4)$ NO_2 + $CF(4)$ HO_2 + $CF(4)$ ALD2	$2.91E-12 \times EXP(180.2/TEMP)$	11
123	$RO_25 + RO_2T$	$HO_2 + ALD2 + RO_2T + O_2$	k ₉₆	
124	$RO_25 + HO_2$	$HO_2 + OH + ALD2$	k ₉₄	
125	$RO_26 + NO$	$NO_2 + CO_2 + RO_2 + RO_2 T$	1.11E-11 × EXP(180.2/TEMP)	11
126 127	$RO_26 + NO_2 + M$	PAN1 + M	see Table 4 see Table 4	12 12
128	PAN1 $RO_26 + HO_2$	$NO_2 + RO_26 + RO_2T$ $O_3 + ACID$	k_{94}	12
129	$RO_26 + RO_2T$	$CO_2 + RO_25 + 2 RO_2T + O_2$	k_{96}	
130	$RO_27 + NO$	$NO_2 + ALD2 + RO_28 + RO_2T$	k ₁₁₃	
131	$RO_2^27 + RO_2T$	$ALD2 + RO_28 + 2 RO_2T + O_2$	k ₉₆	
132	$RO_27 + HO_2$	$OH + ALD2 + RO_28 + RO_2T$	k ₉₄	
133	$RO_28 + NO$	$NO_2 + CO_2 + RO_21 + RO_2T$	k_{125}	
134	$RO_28 + NO_2 + M$	PAN2 + M	k_{126}	
135	PAN2	$NO_2 + RO_28 + RO_2T$	k ₁₂₇	
136 137	$RO_28 + HO_2$ $RO_28 + RO_2T$	$O_3 + ACID$ $CO_2 + RO_21 + 2 RO_2T + O_2$	k ₉₄ k ₉₆	
138	$RO_29 + NO$	CF(5) OLEL + CF(6) NO ₂ + CF(6) HO ₂ + CF(6) HCHO + CF(6) MVK	$2.08E-12 \times EXP(180.2/TEMP)$	11
139	$RO_29 + RO_2T$	$HO_2 + MVK + HCHO + RO_2T$ + O_2	k ₉₆	
140	$RO_29 + HO_2$	$HO_2 + OH + MVK + HCHO$	k ₉₄	
141	$RO_210 + NO$	$NO_2 + HO_2 + HCHO + MCR$	k_{138}	
142	$RO_210 + RO_2T$	$HO_2 + HCHO + MCR + RO_2T + O_2$	k_{96}	
143	$RO_210 + HO_2$	$HO_2 + OH + HCHO + MCR$	k ₉₄	
144	$RO_211 + NO$	$2 \text{ NO}_2 + \text{HCHO} + \text{MVK}$	k_{138}	
145	$RO_211 + RO_2T$	$NO_2 + HCHO + MVK + RO_2T + O_2$	k_{96}	
146	$RO_211 + HO_2$	$NO_2 + OH + HCHO + MVK$	k ₉₄	
147	$RO_212 + NO$	$2 \text{ NO}_2 + \text{HCHO} + \text{MCR}$	k_{138}	
148	$RO_212 + RO_2T$	$NO_2 + HCHO + MCR + RO_2T + O_2$	k ₉₆	
149	$RO_212 + HO_2$	$NO_2 + OH + HCHO + MCR$	k ₉₄	
150	$RO_213 + NO$	$NO_2 + HCHO + RO_239 + RO_2T$	k_{113}	
151	$RO_213 + RO_2T$	$HCHO + RO_239 + 2 RO_2T + O_2$	k ₉₆	
152	$RO_213 + HO_2$	$HCHO + OH + RO_239 + RO_2T$	k ₉₄	
153 154	$RO_239 + NO_1 + M$	$NO_2 + CO_2 + RO_214 + RO_2T$ PAN3 + M	k ₁₂₅	
154	$RO_239 + NO_2 + M$ PAN3	$NO_2 + RO_239 + RO_2T$	k ₁₂₆	
156	$RO_239 + HO_2$	$O_3 + 0.5 \text{ OLEL} + 0.5 \text{ ACID}$	$rac{k_{127}}{k_{94}}$	
157	$RO_239 + RO_2T$	$CO_2 + RO_2 14 + 2 RO_2 T + O_2$	k ₉₆	
158	RO_2 14 + NO	$CF(7)$ OLEL + $CF(8)$ NO_2	k_{122}	
		$+ CF(8) RO_27 + CF(8) RO_2T$		
159	$RO_214 + RO_2T$	$RO_27 + 2 RO_2T + O_2$	k ₉₆	
160	$RO_214 + HO_2$	$OH + RO_27 + RO_2T$	k ₉₄	

Table 2. (continued)

Reaction	Reactants	Products	Rate Constants, a cm molecule s -1	References,
				Comments
161	$RO_215 + NO$	$NO_2 + HO_2 + CF(9)$ ALD2	k_{138}	
		+ CF(10) HCHO + CF(11) KETL + CF(12) ALKL		
162	$RO_215 + RO_2T$	$HO_2 + CF(13) ALD2 + CF(14)$	k ₉₆	
	2 2	HCHO + CF(15) KETL	70	
		+ CF(16) ALKL + RO2T + O2		
163	$RO_215 + HO_2$	$OH + HO_2 + CF(13) ALD2$	k_{94}	
		+ CF(14) HCHO + CF(15) KETL + CF(16) ALKL		
164	$RO_216 + NO$	$NO_2 + ALD2 + RO_28 + RO_2T$	$1.48E-12 \times EXP(180.2/TEMP)$	11
165	$RO_216 + RO_2T$	$ALD2 + RO_28 + 2 RO_2T + O_2$	k_{96}	
166	$RO_216 + HO_2$	$OH + ALD2 + RO_28 + RO_2T$ $OF(21) AP1 + OF(22) NO$	k ₉₄	11
167	$RO_217 + NO$	$CF(21) AP1 + CF(22) NO_2$ + $CF(22) HO_1 + CF(22) PPP2$	$1.25E-12 \times EXP(180.2/TEMP)$	11
168	$RO_217 + RO_2T$	$+ CF(22) HO_2 + CF(22) RPR2$ $+ HO_2 + RPR2 + RO_2T + O_2$	k ₉₆	
169	$RO_217 + HO_2$	$HO_2 + OH + RPR2$	k ₉₄	
170	$RO_218 + NO$	$CF(19) AP2 + CF(20) NO_2$	k_{167}	
	DO 40 - DO 5	$+ CF(20) HO_2 + CF(20) UR16$		
171 172	$RO_218 + RO_2T$	$HO_2 + UR16 + RO_2T + O_2$ $HO_2 + OH + UR16$	k ₉₆	
173	$RO_218 + HO_2$ $RO_219 + NO$	$2 \text{ NO}_2 + \text{HCHO} + \text{RPR1}$	k_{94} 1.05E-12 × EXP(180.2/TEMP)	11
174	$RO_219 + RO_2T$	$NO_2 + HCHO + RPR1 + RO_2T$	k_{96}	
		$+$ O_2		
175	$RO_219 + HO_2$	$NO_2 + OH + HCHO + RPR1$	k_{94}	
176	$RO_220 + NO$	$CF(17) AP3 + CF(18) NO_2$ + $CF(18) PO_118 + CF(18) PO_17$	k ₁₆₇	
177	$RO_220 + RO_2T$	$+ CF(18) RO_218 + CF(18) RO_2T$ $RO_218 + 2 RO_2T + O_2$	k ₉₆	
178	$RO_220 + HO_2$	$OH + RO_218 + RO_2T$	k_{94}	
179	$RO_221 + NO$	$CF(23) AP4 + CF(24) NO_2$	k_{173}	
100	DO 21 + DO T	$+ CF(24) HO_2 + CF(24) ARAL$,	
180 181	$RO_221 + RO_2T$ $RO_221 + HO_2$	$HO_2 + ARAL + RO_2T + O_2$ $HO_2 + OH + ARAL$	$k_{96} = k_{94}$	
182	$RO_221 + RO_2$ $RO_222 + NO$	$CF(41) AP5 + CF(42) NO_2$	k_{167}	
		$+ CF(42) HO_2 + CF(42) RPR6$	107	
183	$RO_222 + RO_2T$	$HO_2 + RPR6 + RO_2T + O_2$	k_{96}	
184	$RO_222 + HO_2$	$HO_2 + OH + RPR6$	k_{94}	
185	$RO_223 + NO$	CF(43) AP6 + CF(44) NO ₂ + CF(44) HO ₂ + CF(44) RPR7	k ₁₆₇	
186	$RO_223 + RO_2T$	$HO_2 + RPR7 + RO_2T + O_2$	k ₉₆	
187	$RO_223 + HO_2$	$HO_2 + OH + RPR7$	k ₉₄	
188	$RO_224 + NO$	$CF(25) AP7 + CF(26) NO_2$	$8.89E-13 \times EXP(180.2/TEMP)$	11
100	DO 24 + DO T	$+ CF(26) HO_2 + CF(26) RPR3$	I.	
189 190	$RO_224 + RO_2T$ $RO_224 + HO_2$	$HO_2 + RPR3 + RO_2T + O_2$ $HO_2 + OH + RPR3$	k ₉₆ k ₉₄	
191	$RO_225 + NO$	$2 \text{ NO}_2 + \text{RPR3}$	k_{188}	
192	$RO_2^225 + RO_2T$	$NO_2 + RPR3 + RO_2T + O_2$	k_{96}	
193	$RO_225 + HO_2$	$NO_2 + OH + RPR3$	k_{94}	
194	$RO_226 + NO$	$NO_2 + UR17 + RO_28 + RO_2T$	k_{188}	
195 196	$RO_226 + RO_2T$ $RO_226 + HO_2$	$UR17 + RO_28 + 2 RO_2T + O_2$ $UR17 + OH + RO_28 + RO_2T$	k ₉₆ k ₉₄	
197	$RO_220 + NO_2$ $RO_227 + NO_2$	$CF(27) AP8 + CF(28) NO_2$	k_{188}	
	2	$+ CF(28) HO_2 + CF(28) UR7$	100	
198	$RO_227 + RO_2T$	$HO_2 + UR7 + RO_2T + O_2$	k_{96}	
199	$RO_227 + HO_2$	$HO_2 + OH + UR7$	k_{94}	
200 201	$RO_228 + NO$ $RO_228 + RO_2T$	$2 \text{ NO}_2 + \text{UR7}$ $\text{NO}_2 + \text{UR7} + \text{RO}_2\text{T} + \text{O}_2$	$rac{k_{188}}{k_{96}}$	
202	$RO_228 + RO_21$ $RO_228 + HO_2$	$NO_2 + OR + RO_2 I + O_2$ $NO_2 + OH + UR7$	n ₉₆ k ₉₄	
203	$RO_229 + NO$	$CF(29) AP9 + CF(30) NO_2$	k_{173}	
		$+ CF(30) RO_240 + CF(30) RO_2T$		
204	$RO_229 + RO_2T$	$RO_240 + 2 RO_2T + O_2$	k ₉₆	
205	$RO_229 + HO_2$	$OH + RO_240 + RO_2T$	k ₉₄	
206 207	$RO_240 + NO$ $RO_240 + RO_2T$	NO ₂ + RPR8 + RO ₂ 8 + RO ₂ T RPR8+ RO ₂ 8 + 2 RO ₂ T + O ₂	k ₁₇₃ k ₉₆	
208	$RO_240 + HO_2$	OH + RPR8 + RO28 + RO2T	k_{94}	
209	$RO_230 + NO$	$NO_2 + UR18 + RO_28 + RO_2T$	k_{188}	
210	$RO_230 + RO_2T$	$UR18 + RO_28 + 2 RO_2T + O_2$	k ₉₆	
211	$RO_230 + HO_2$	OH + UR18 + $RO_28 + RO_2T$ CE(31) AP10 + CE(32) NO	k_{94} 6.32F 13 × EYD(180.2/TEMD)	11
212	$RO_231 + NO$	$CF(31) AP10 + CF(32) NO_2 + CF(32) HO_2 + CF(32) UR19$	$6.32E-13 \times EXP(180.2/TEMP)$	11
213	$RO_231 + RO_2T$	$HO_2 + UR19 + RO_2T + O_2$	k ₉₆	
214	$RO_231 + HO_2$	$HO_2 + OH + UR19$	k ₉₄	

Table 2. (continued)

Reaction	Reactants	Products	Rate Constants, ^a cm molecule ⁻¹ s ⁻¹	References, Comments
215	RO ₂ 32 + NO	CF(33) AP11 + CF(34) NO ₂ + CF(34) RO ₂ 41 + CF(34) RO ₂ T	3.2E-13 × EXP(180.2/TEMP)	11
216	$RO_232 + RO_2T$	$RO_241 + 2 RO_2T + O_2$	k ₉₆	
217	$RO_232 + HO_2$	$OH + RO_241 + RO_2T$	k_{94}	
218	$RO_241 + NO$	CF(35) AP12 + CF(36) NO ₂ + CF(36) HO ₂ + CF(36) UR20	k_{215}	
219	$RO_241 + RO_2T$	$HO_2 + UR20 + RO_2T + O_2$	k ₉₆	
220	$RO_241 + HO_2$	$HO_2 + OH + UR20$	k ₉₄	12
221	RO_233	$RO_242 + RO_2T$	$1.64E+42/TEMP^{11.4} \times EXP (-9460/TEMP)$	13
222	$RO_233 + NO$	$NO_2 + HO_2 + RPR9$	<i>k</i> ₁₆₇	
223	$RO_233 + RO_2T$	$HO_2 + RPR9 + RO_2T + O_2$	k ₉₆	
224 225	$RO_233 + HO_2$	$HO_2 + OH + RPR9$	k ₉₄	
226	RO242 + NO RO242 + RO2T	$NO_2 + HO_2 + RP10 + MGLY$ $HO_2 + RP10 + MGLY + O_2$	k ₁₆₇ k ₉₆	
227	$RO_242 + HO_2$	+ RO2T HO2 + OH + RP10 + MGLY	k ₉₄	
228	RO ₂ 34	$RO_243 + RO_2T$	k_{221}	
229	$RO_234 + NO$	$NO_2 + HO_2 + RP11$	k_{173}	
230	$RO_234 + RO_2T$	$HO_2 + RP11 + RO_2T + O_2$	k ₉₆	
231	$RO_234 + RO_21$ $RO_234 + HO_2$	$HO_2 + OH + RP11$	k ₉₄	
232	$RO_243 + NO$	$NO_2 + HO_2 + RP10 + MGLY$	k_{173}	
233	$RO_243 + RO_2T$	$HO_2 + RP10 + MGLY + O_2 + RO_2T$	k_{96}	
234	$RO_243 + HO_2$	$HO_2 + OH + RP10 + MGLY$	k_{94}	
235	RO ₂ 35	$RO_244 + RO_2T$	k_{221}	
236	$RO_235 + NO$	$NO_2 + HO_2 + RP11$	k ₁₈₈	
237	$RO_235 + RO_2T$	$HO_2 + RP11 + RO_2T + O_2$	k ₉₆	
238	$RO_235 + HO_2$	$HO_2 + OH + RP11$	k ₉₄	
239	$RO_244 + NO$	$NO_2 + HO_2 + RP10 + MGLY$	k_{188}	
240	$RO_244 + RO_2T$	$HO_2 + RP10 + MGLY + O_2$ + RO_2T	k_{96}	
241	$RO_244 + HO_2$	$HO_2 + OH + RP10 + MGLY$	k_{94}	
242	RO ₂ 36	$RO_245 + RO_2T$	k_{221}	
243	$RO_236 + NO$	$NO_2 + HO_2 + RP12$	k_{167}	
244	$RO_236 + RO_2T$	$HO_2 + RP12 + RO_2T + O_2$	k ₉₆	
245	$RO_2^236 + HO_2^2$	$HO_2 + OH + RP12$	k ₉₄	
246	$RO_245 + NO$	$NO_2 + HO_2 + RP10 + MGLY$	k ₁₆₇	
247	$RO_245 + RO_2T$	$HO_2 + RP10 + MGLY + O_2 + RO_2T$	k ₉₆	
248	$RO_245 + HO_2$	$HO_2 + OH + RP10 + MGLY$	k_{94}	
249	RO ₂ 37	$RO_246 + RO_2T$	k_{221}	
250	$RO_2^237 + NO$	$NO_2 + HO_2 + RP13$	k_{167}	
251	$RO_2^237 + RO_2T$	$HO_2 + RP13 + RO_2T + O_2$	k_{96}	
252	$RO_{2}37 + HO_{2}$	$HO_2 + OH + RP13$	k ₉₄	
253	$RO_246 + NO$	$NO_2 + HO_2 + RP10 + MGLY$	k_{167}	
254	$RO_2^246 + RO_2T$	$HO_2 + RP10 + MGLY + O_2 + RO_2T$	k_{96}	
255	$RO_246 + HO_2$	$HO_2 + OH + RP10 + MGLY$	k ₉₄	
256	RO ₂ 38	$RO_247 + RO_2T$	k_{221}	
257	$RO_238 + NO$	$NO_2 + HO_2 + RP14$	k_{212}	
258	$RO_238 + RO_2T$	$HO_2 + RP14 + RO_2T + O_2$	k ₉₆	
259	$RO_238 + HO_2$	$HO_2 + OH + RP14$	k_{94}	
260	$RO_247 + NO$	$NO_2 + HO_2 + RP15 + MGLY$	k_{212}	
261	$RO_247 + RO_2T$	$\begin{array}{l} \mathrm{HO_2} + \mathrm{RP15} + \mathrm{MGLY} + \mathrm{O_2} \\ + \mathrm{RO_2T} \end{array}$	k_{96}	
262	$RO_247 + HO_2$	$HO_2 + OH + RP15 + MGLY$	k ₉₄	
263	MGLY + OH	$RO_2^248 + RO_2T + H_2O$	1.72E-11	5
264	$MGLY + NO_3$	$HNO_3 + RO_248 + RO_2T$	$1.4E-12 \times EXP(-1897.3/TEMP)$	2
265	MGLY + hv	$CO + HO_2 + RO_28 + RO_2T$	see Table 3	1
266	$RO_248 + NO$	$NO_2 + CO_2 + RO_28 + RO_2T$	k_{125}	
267	$RO_2^248 + NO_2 + M$	PAN4 + M	k_{126}	
268	PAN4	$NO_2 + RO_248 + RO_2T$	k_{127}	
269	$RO_248 + HO_2$	$O_3 + UR21$	k ₉₄	
270	$RO_2^248 + RO_2^2T$	$CO_2 + RO_28 + 2 RO_2T + O_2$	k ₉₆	
271	MVK + OH	$RO_249 + RO_2T$	$4.14E-12 \times EXP(452.9/TEMP)$	2
272	$MVK + O_3$	0.56 CO + 0.2 CO ₂ + 0.28 HO ₂ + 0.36 OH + 0.5 MGLY + 0.5 HCHO + 0.12 ACID + 0.1 ALD2 + 0.12 UR21 + 0.28 RO ₂ 8 + 0.28 RO ₂ T + 0.2 H ₂ O	7.5E-16 × EXP(-1519.9/TEMP)	2
273	MVK + O	$0.85 \text{ KETL} + 0.15 \text{ RO}_24$	4.32E-12	2

Table 2. (continued)

Reaction	Reactants	Products	Rate Constants, a cm molecule 1 s -1	References, Comments
274 275	$RO_249 + NO$ $RO_249 + RO_2T$	$NO_2 + HO_2 + MGLY + HCHO$ $HO_2 + MGLY + HCHO + RO_2T$ $+ O_2$	k ₁₁₃ k ₉₆	
276 277	$RO_249 + HO_2$ MCR + OH	HO ₂ + OH + MGLY + HCHO CF(46) RO ₂ 50 + CF(46) H ₂ O + CF(47)	k_{94} 1.86E-11 × EXP(176.1/TEMP)	2
278	MCR + NO ₃	$RO_251 + RO_2T$ $CF(46) HNO_3 + CF(46) RO_250 +$	$1.5E-12 \times EXP(-1726.2/TEMP)$	2
279	$MCR + O_3$	CF(47) RO ₂ 52 + RO ₂ T 0.41 CO + 0.41 HO ₂ + 0.82 OH + 0.5 HCHO + 0.59 MGLY + 0.09 ACID +	$1.36E-15 \times EXP(-2113.7/TEMP)$	2
280	MCR + O	0.41 RO ₂ 53 + 0.41 RO ₂ T 0.15 CO + 0.15 HO ₂ + 0.85 ALD2 + 0.15 RO ₂ 7 + 0.15 RO ₂ T	6.34E-12	2
281	$RO_250 + NO$	$CO_2 + NO_2 + RO_2 I + RO_2 T$	k_{125}	
282	$RO_250 + NO_2 + M$	PAN5 + M	k_{126}	
283	PAN5	$NO_2 + RO_2 50 + RO_2 T$	k_{127}	
284	$RO_250 + HO_2$	$O_3 + 0.5 \text{ ACID} + 0.5 \text{ OLEL}$	k ₉₄	
285	$RO_2^250 + RO_2^2T$	$CO_2 + RO_214 + 2 RO_2T + O_2$	k ₉₆	
286	$RO_251 + NO$	$NO_2 + HO_2 + HCHO + MGLY$	k_{113}	
287	$RO_251 + HO_2$	$HO_2 + HCHO + MGLY + RO_2T + O_2$	k_{94}	
288	$RO_251 + RO_2T$	$HO_2 + OH + MGLY + HCHO$	k ₉₆	
289	$RO_252 + NO$	$2 \text{ NO}_2 + \text{MGLY} + \text{HCHO}$	k_{113}	
290	$RO_252 + HO_2$	$NO_2 + MGLY + HCHO + RO_2T + O_2$	k_{94}	
291	$RO_252 + RO_2T$	$NO_2 + OH + MGLY + HCHO$	k ₉₆	
292	$RO_253 + NO$	$NO_2 + HCHO + RO_254 + RO_2T$	k ₁₂₂	
293	$RO_253 + HO_2$	$HCHO + RO_254 + 2 RO_2T + O_2$	k ₉₄	
294 295	$RO_253 + RO_2T$ $RO_254 + NO$	$OH + HCHO + RO_254 + RO_2T$ $CO_2 + CO + NO_2 + HO_2$	k96	
296	$RO_254 + NO_2 + M$	PAN6 + M	$k_{125} \\ k_{126}$	
297	PAN6	$NO_2 + RO_254 + NO_2$	k ₁₂₇	
298	$RO_254 + HO_2$	$O_3 + RP16$	k ₉₄	
299	$RO_254 + RO_2T$	$CO_2 + CO + HO_2 + RO_2T + O_2$	k ₉₆	
300	RPR1 + OH	$RO_255 + RO_2T + H_2O$	see Table 6	8
301	$RPR1 + NO_3$	$HNO_3 + RO_255 + RO_2T$	$k_{61} \times k_{300}/k_{60}$	estimated k
302	RPR1 + hv	$CO + HO_2 + RO_2 20 + RO_2 T$	see Table 3	1
303	$RO_255 + NO$	$NO_2 + CO_2 + RO_2 20 + RO_2 T$	k_{125}	
304	$RO_255 + NO_2 + M$	PAN7 + M	k ₁₂₆	
305	PAN7	$NO_2 + RO_255 + RO_2T$	k ₁₂₇	
306 307	$RO_255 + HO_2$	$O_3 + UR1$ $CO_2 + RO_2 20 + 2 RO_2 T + O_2$	k ₉₄	
308	$RO_255 + RO_2T$ RPR2 + OH	$O_3 - HO_2 + UR2 + H_2O$	$k_{96} = k_{82}$	
309	RPR3 + OH	$RO_256 + RO_2T + H_2O$	see Table 6	8
310	$RPR3 + NO_3$	$HNO_3 + RO_256 + RO_2T$	$k_{61} \times k_{309}/k_{60}$	estimated k
311	RPR3 + hv	$CO + 2 HO_2 + UR4$	see Table 3	1
312	$RO_256 + NO$	$NO_2 + CO_2 + HO_2 + UR4$	k_{125}	
313	$RO_2^256 + NO_2 + M$	PAN8 + M	k_{126}	
314	PAN8	$NO_2 + RO_256 + RO_2T$	k_{127}	
315	$RO_256 + HO_2$	$O_3 + UR3$	k_{94}	
316	$RO_256 + RO_2T$	$CO_2 + HO_2 + UR4 + RO_2T + O_2$	k_{96}	_
317	$RPR4 + NO_3$	$HNO_3 + RAD8$	3.77E-12	2
318	$RAD8 + NO_2$	$UR22 + H_2O$	$2.30E-11 \times EXP(151.0/TEMP)$	2
319 320	RPR5 + OH RPR6 + OH	$O_3 - HO_2 + UR14 + H_2O$ $O_3 - HO_2 + RPR7 + H_2O$	k_{82}	
320	RPR7 + OH	$O_3 - HO_2 + KFK7 + H_2O$ $O_3 - HO_2 + ADAC + H_2O$	$k_{82} \ k_{82}$	
322	RPR8 + OH	$RO_257 + RO_2T + H_2O$	see Table 6	8
323	$RPR8 + NO_3$	$HNO_3 + RO_257 + RO_2T$	$k_{61} \times k_{322}/k_{60}$	estimated k
324	RPR8 + hv	$CO + HO_2 + RO_29 + RO_2T$	see Table 3	1
325	RPR8 + hv	$HO_2 + RO_257 + RO_2T$	see Table 3	1
326	$RO_257 + NO$	$NO_2 + CO_2 + RO_29 + RO_2T$	k_{125}	
327	$RO_257 + NO_2$	PAN9	k_{126}	
328	PAN9	$NO_2 + RO_257 + RO_2T$	k_{127}	
329	$RO_257 + HO_2$	$UR23 + O_3$	k ₉₄	
330	$RO_257 + RO_2T$	$CO_2 + RO_29 + 2 RO_2T + O_2$	k ₉₆	o
331 332	RPR9 + OH RP10 + OH	$O_3 - HO_2 + RP17 + H_2O$ $HO_2 + UR24 + H_2O$	see Table 6 see Table 6	8 8
333	RP10 + OH RP10 + hv	$HO_2 + UR24 + H_2O$ UR25	see Table 6 see Table 3	1
334	RP11 + OH	$O_3 - HO_2 + UR26 + H_2O$	see Table 6	8
	RP12 + OH	$O_3 - HO_2 + RP13 + H_2O$	see Table 6	8
333				8
335 336	RP13 + OH	$O_3 - HO_2 + RP18 + H_2O$	see Table 6	0
	RP13 + OH RP14 + OH	$O_3 - HO_2 + RP18 + H_2O$ $O_3 - HO_2 + RP19 + H_2O$	see Table 6	8
336				

Table 2. (continued)

Reaction	Reactants	Products	Rate Constants, a cm molecule s -1	References, Comments
340	$RP16 + NO_3$	$HNO_3 + RO_258 + RO_2T$	k ₂₆₄	
341	RP16 + hv	$2 \text{ CO} + \text{OH} + \text{HO}_2$	see Table 3	1
342	$RO_258 + NO$	$CO + CO_2 + NO_2 + OH$	k_{125}	
343	$RO_{2}58 + NO_{2} + M$	PN10 + M	k_{126}	
344	PN10	$NO_2 + RO_258 + RO_2T$	k_{127}	
345	$RO_258 + HO_2$	$O_3 + UR28$	k_{94}	
346	$RO_258 + RO_2T$	$CO + CO_2 + OH + RO_2T + O_2$	k_{96}	
347	RP17 + OH	$O_3 - HO_2 + UR29 + H_2O$	see Table 6	8
348	RP18 + OH	$O_3 - HO_2 + UR30 + H_2O$	see Table 6	8
349	RP19 + OH	$O_3 - HO_2 + UR31 + H_2O$	see Table 6	8
350	AP1 + OH	$NO_2 + RPR2 + H_2O$	see Table 6	8
351	AP2 + OH	$NO_2 + UR16 + H_2O$	see Table 6	8
352	AP3 + OH	$NO_2 + UR32 + H_2O$	see Table 6	8
353	AP4 + OH	$NO_2 + ARAL + H_2O$	see Table 6	8
354	AP5 + OH	$NO_2 + RPR6 + H_2O$	see Table 6	8
355	AP6 + OH	$NO_2 + RPR7 + H_2O$	see Table 6	8
356	AP7 + OH	$NO_2 + RPR3 + H_2O$	see Table 6	8
357	AP8 + OH	$NO_2 + UR7 + H_2O$	see Table 6	8
358	AP9 + OH	$NO_2 + UR33 + H_2O$	see Table 6	8
359	AP10 + OH	$NO_2 + UR19 + H_2O$	see Table 6	8
360	AP11 + OH	$NO_2 + UR34 + H_2O$	see Table 6	8
361	AP12 + OH	$NO_2 + UR20 + H_2O$	see Table 6	8

^a If reaction rates depend on concentrations of M or O₂, these rate constants already take this into account by multiplying by the appropriate factor. The host model requires rate constants in ppm min⁻¹ units. For example, to convert from cm³ molecule⁻¹ s⁻¹ to ppm⁻¹ min⁻¹, multiply by 4.4E+17/TEMP. The CF(i) factors represent product stoichiometric yields estimated or determined kinetically: CF(1), CF(2), CF(39), CF(40), and CF(45) - CF(47) [Kwok and Atkinson, 1995]; CF(9)-CF(16) [Japar et al., 1990]; and all others [Carter and Atkinson, 1989]. Rate constant references: 1, Harley et al. [1993]/ Lurmann et al. [1987]; 2, Carter/SAPRC-97 and Carter/SAPRC-99; 3, Dransfield et al. [1999]; 4, Atkinson [1994]; 5, Atkinson [1997]; 6, Atkinson [1990]; 7, Japar et al. [1990]; 8, Kwok and Atkinson [1995]; 9, Hoffmann et al. [1997]; 10, Goumri et al. [1992]; 11, Jenkin et al. [1997]; 12, Stockwell et al. [1997]; 13, Lay et al. [1996].

result is RO₂18, a hydroxy alkyl peroxy radical, that can react like other peroxy radicals (reactions 170-172) to form a hydroxy alkyl nitrate (AP2), HO₂, and a hydroxy ketone (UR16). (Products that are considered nonreactive or whose oxidation products do not have vapor pressures estimated to be an order of magnitude less than the first product itself are labeled as unreactive, URi; such species are assumed to have a first-order loss coefficient of 10^{-3} min⁻¹ in order to prevent excessive build-up of these compounds). In this case, the alkyl nitrate products have sufficiently high carbon number that they or their oxidation products could potentially participate in SOA formation. The oxidation of such alkyl nitrate products proceeds by OH abstraction of the Hatom closest to the nitrooxy group. Subsequent decomposition reactions and reactions with O2 result in the release of NO₂ and formation of functionalized products. In the case of AP2 (reaction 351), UR16 is assumed to form. In the case of AP3 (reaction 352), a ketone (UR32) is formed.

Table 3. Photolysis Rate Constants (Shown for 3PM 1500 LT, 27 August 1987 in Los Angeles, 34.058°N, 118.25°W)^a

Photolyzed Species (Reaction Number)	Products	Typical Value of j_i , s^{-1}	Comments
NO ₂ (1)	NO + O	6.68E-3	
NO_3^2 (13)	$NO + O_2$	1.65E-2	
$NO_3(14)$	$NO_2 + O$	1.45E-1	
$O_3(15)$	$O + O_2$	3.90E-4	
$O_3(16)$	$OSD + O_2$	1.66E-5	
HONO (20)	$0.9 \text{ NO} + 0.1 \text{ NO}_2 + 0.1 \text{ HO}_2$	1.30E-3	
	+ 0.9 OH		
H_2O_2 (36)	2 OH	5.07E-6	
HCHO (44)	$HO_2 + CO$	1.97E-5	
HCHO (45)	$CO + H_2$	3.38E-5	
ALD2 (59)	$CO + HO_2 + RO_25 + RO_2T$	4.45E-6	
KETL (63)	$RO_25 + RO_28 + 2 RO_2T$	9.37E-7	
KETH (71)	$RO_{2}^{2}5 + RO_{2}^{2}8 + 2 RO_{2}^{2}T$	9.37E-7	assumed equal to j_{KETL}
MGLY (265)	$CO + HO_2 + RO_28 + RO_2T$	1.32E-4	1 311212
RPR1 (302)	$CO + HO_2 + RO_2 20 + RO_2 T$	4.45E-6	assumed equal to j_{ALD2}
RPR3 (311)	$CO + 2 HO_2 + UR4$	4.45E-6	assumed equal to j_{ALD2}
RPR8 (324)	$CO + HO_2 + RO_29 + RO_2T$	4.45E-6	assumed equal to i_{ALD2}
RPR8 (325)	$HO_2 + RO_257 + RO_2T$	4.45E-6	assumed equal to j_{ALD2}
RP10 (333)	UR25	4.45E-6	assumed equal to j_{ALD2}
RP16 (341)	$CO + OH + HO_2$	1.32E-4	assumed equal to j_{MGLY}

^a Photolysis rate constants as a function of zenith angle are calculated by integrating over ultraviolet wavelengths the product (actinic irradiance times absorption cross section times quantum yield). Zenith angles are geometrically calculated based on the percentage of daylight that has passed. Cross sections and quantum yields are described by McRae [1981] and Lurmann et al. [1987].

Table 4. Three-Body Kinetics Rate Constant Calculations^a

Reactio	n k_0^{300}	n	$k_{\rm inf}^{300}$	m	F
4	9.0E-32	2	2.2E-11	0	0.8
9	2.8E-30	3.5	2.0E-12	0.2	0.45
10	equilibrium with (9)				
19	7.0E-31	2.6	3.6E-11	0.1	0.6
22^{b}	2.85E-30	2.67	3.13E-11	0	see footnote
27	1.8E-31	3.2	4.7E-12	0	0.6
28	equilibrium with (27)				
35	4.1E-31	3.3	2.0E-12	0	0.45
126	9.7E-29	5.6	9.3E-12	1.5	0.6
127	equilibrium with (126)				

^aThree-body rate constants at temperature T (K) and pressure corresponding to [M] (molecule cm⁻³) are found via the following formulae:

$$\begin{split} k_o(T) &= k_o^{300}(T) \bigg(\frac{T}{300}\bigg)^{-n} \big(\text{cm}^6 \text{ molecule}^{-2} \text{ s}^{-1}\big), \\ k_{inf}(T) &= k_{\text{inf}}^{300}(T) \bigg(\frac{T}{300}\bigg)^{-m} \big(\text{cm}^3 \text{ molecule}^{-1} \text{ s}^{-1}\big), \\ k(T,z) &= \bigg(\frac{k_o(T)[M]}{1 + (k_o(T)[M]/k_{\text{inf}}(T))}\bigg) F^{(1+[\log_{10}(k_0(T)[M]/k_{\text{inf}}(T))])^{-1}} \end{split}$$

$$(cm^3 molecule^{-1} s^{-1}).$$

^bThe rate constant expression for reaction 22 has small correction factors incorporated into it. It is found as given by *Dransfield et al.* [1999].

3.1.3. Long Chain Alkanes

[14] Long chain alkanes (ALKH) are represented by nhexadecane since hexadecane exhibits the approximate average number of carbons of those long chain n-alkanes that reside at least partially in the gas phase. Oxidation proceeds as above (reaction 93) and results in the formation of RO₂32, which is formed only from the oxidation of ALKH and is represented by 8-hexadecyl peroxy radical. Reaction of RO₂32 (reactions 215-217) forms either 8hexadecyl nitrate (AP11) or RO₂41 (8-hydroxy-11-hexadecyl-peroxy radical) via the 1,5-H shift. RO₂41 (reactions 218-220) forms either 8-hydroxy-11-hexadecyl nitrate (AP12) or 11-hydroxy-8-hexadecanone (UR20) via a second isomerization and reaction with O₂. Oxidation of AP11 and AP12 (reactions 360 and 361) results in the formation of the corresponding carbonyls (UR34 and UR20, respectively). The chemistry of ALKH is shown in Figure 1a.

3.2. Nonbiogenic Alkenes

3.2.1. Ethene

[15] Despite their high reactivity [Atkinson, 1997], alkenes are still found in high concentration in the ambient [Fraser et al., 1997], which is indicative of significant emissions [Schauer, 1998; Schauer et al., 1999a, 1999b].

Table 6. Hydroxyl Radical Rate Constants Calculated Using a Structure-Reactivity Relationship^a

Reaction	$k \times 10^{10}$ (cm ³ molecule ⁻¹ s ⁻¹) at 300 K	Reaction	$k \times 10^{10}$ (cm ³ molecule ⁻¹ s ⁻¹) at 300 K
69 (ALCH)	0.128	338 (RP15)	0.130
70 (KETH)	0.051	347 (RP17)	2.195
73 (AROO)		348 (RP18)	1.970
74 (OLEH)	0.347	349 (RP19)	1.336
78 (ALKM)	0.103	350 (AP1)	2.202
80 (AROH)	0.152	351 (AP2)	0.054
83 (ARAC)	0.011	352 (AP3)	0.077
93 (ALKH)	0.197	353 (AP4)	0.331
300 (RPR1)	0.354	354 (AP5)	0.132
309 (RPR3)	0.424	355 (AP6)	0.014
322 (RPR8)	1.145	356 (AP7)	0.305
331 (RPR9)	2.414	357 (AP8)	1.030
332 (RP10)	1.098	358 (AP9)	0.907
334 (RP11)	1.964	359 (AP10)	0.777
335 (RP12)	2.407	360 (AP11)	0.188
336 (RP13)	2.189	361 (AP12)	0.278
337 (RP14)	1.452		

^aAs shown by *Kwok and Atkinson* [1995], the rate constant for OH oxidation of an organic species is dependent on the number and type of structural components and the location of these groups relative to other groups. For example, ALKH is represented by *n*-hexadecane. There are three types of structural components associated with this molecule: $-\text{CH}_3$ positioned next to $-\text{CH}_2$ -(2), $-\text{CH}_2$ -positioned between $-\text{CH}_3$ and $-\text{CH}_2$ -(2), and $-\text{CH}_2$ -positioned between other $-\text{CH}_2$ - (14). The rate constant of ALKH is found from $k_{ALKH} = 2k_{CH_3}f_{CH_2} + 2k_{CH_2}f_{CH_3}f_{CH_2} + 14k_{CH_2}f_{CH_2}^2$ where k_i represents a rate constant for group i and f_i represents a temperature dependent substituent factor. In this case, $k_{CH_3} = 4.49 \times 10^{-18} \, T^2 e^{-320/T}$ (cm³ molecule⁻¹ s⁻¹), $k_{CH_2} = 4.50 \times 10^{-18} \, T^2 e^{-253/T}$ (cm³ molecule⁻¹ s⁻¹), $f_i = e^{E_i/T}$ (dimensionless), $E_{CH_3} = 0$ (K), and $E_{CH_2} = 61.69$ (K). The parameters for k_i and f_i for unsaturated bonds and most functional groups also exist.

Given that its atmospheric chemistry is relatively well understood [Atkinson, 1997], ethene (ETHE) is treated explicitly. Reaction of alkenes with OH, NO₃, O₃, and $O(^{3}P)$ (reactions 49–52, respectively, for ETHE) are taken into account. In the case of ETHE, addition of OH results in the formation of RO₂2, a lumped 2-hydroxy, 4-carbon, primary peroxy radical, that can undergo peroxy radical reactions similar to those described in the alkanes section above (reactions 113-115). However, in the case of the NO reaction, an alkyl nitrate product is not formed because of the small carbon number [Carter and Atkinson, 1989]. Products of these reactions are HCHO, ALD2, and HO₂. Reaction of ETHE with NO₃ proceeds similarly with an ONO_2 group replacing the OH group in the radical (RO_23). The reactions of RO₂3 (reactions 116–118) create HCHO, ALD2, and HO₂; NO₂ is liberated from RO₂3 upon reaction as well. The reaction of ETHE with O₃ is initiated by O₃ attack of the double bond in the well-established bridging mechanism. The decomposition of the highly energetic intermediate leads to formation of a short chain n-carboxylic

Table 5. Other Rate Constant Calculations

Reaction	Expression ^a	k_1	k_2	k_3
23	a	$7.2E-15 \times EXP(785.1/TEMP)$	$4.1E-16 \times EXP(1439.4/TEMP)$	$1.9E-33 \times EXP(724.7/TEMP)$
24	b	1.3E-13	3.19E-33	_
31	b	$2.2E-13 \times EXP(598.9/TEMP)$	$1.85E-33 \times EXP(981.4/TEMP)$	_
32 ^b	b	$3.08E-34 \times EXP(2798.2/TEMP)$	$2.59E-54 \times EXP(3180.7/TEMP)$	

^a Three-body rate constants at temperature TEMP (K) and pressure corresponding to [M] (molecule cm⁻³) are found via the following formulae: (a) $k(\text{cm}^3 \text{ molecule}^{-1} \text{ s}^{-1}) = k_1 + k_2[M]$ or (b) $k(\text{cm}^3 \text{ molecule}^{-1} \text{ s}^{-1}) = k_1 + k_3[M](1 + k_3[M]/k_2)$. ^b Reaction 32 is third order.

Figure 1. An illustrative example of a degradation mechanism for a parent hydrocarbon: (a) ALKH, (b) AROL, and (c) ISOP (see Table 1 and text for notation).

Figure 1. (continued)

acid (ACID), HO₂, CO, OH, HCHO, and H₂O. Yields of these products are shown in Table 2 and are derived from *Jenkin et al.* [1997]. The final reaction of ETHE is that with O(3 P), leading to formation of RO₂1, CO, HO₂, and RO₂4, an aldehydic 2-carbon peroxy radical, with yields shown in Table 2 and derived from *Atkinson* [1997]. RO₂4 acts like other peroxy radicals (reactions 119–121); however, radicals such as RO₂4 that exhibit an α -carbonyl are assumed not to form alkyl nitrate products [*Jenkin et al.*, 1997].

3.2.2. Short Chain Alkenes

[16] Short chain alkenes with three to six carbon atoms (OLEL) are represented by 1-pentene because of the high ambient presence of straight chain α-alkenes. Similar to ETHE, OLEL is consumed by OH, NO₃, O₃, and O(³P) (reactions 54–57). As with ETHE, OH and NO₃ reaction lead to RO₂2 and RO₂3, respectively. OLEL reaction with O₃ leads to formation of HCHO, ALD2, ACID, CO, OH, CO₂, HO₂, ALKL (a reclassified reactive product), and RO₂5 in yields shown in Table 2 and derived from *Jenkin et al.* [1997]. The OLEL reaction with O(³P) leads to ALKL (a reclassified reactive product), ALD2, RO₂4, and RO₂5 in yields also shown in Table 2 and derived from *Atkinson* [1997].

3.2.3. Long Chain Alkenes

[17] Longer chain alkenes (OLEH) are those with seven or more carbon atoms and are represented by 4-methyl-1-octene because of the high ambient presence of branched α -alkenes. As before, OH, NO₃, O₃, and O(3 P) can react with OLEH (reactions 74–77, respectively). Reactions with OH and NO₃ lead to RO₂18 and RO₂19, respectively. The reactions of RO₂18, represented by a lumped structure (2-mehtyl-2-hydroxy-5-heptyl peroxy radical), are described above.

RO₂19 is formed exclusively by OLEH and is the corresponding radical with the nitrooxy group in the 1-position and the peroxy radical at the 2-position. Its reactions (173– 175) result in the formation of HCHO and 3-methyl-heptanal (RPR1) (Reactive products that are capable of participating in SOA formation and that do not exhibit a nitrooxy group are labeled RPRi or RPi.). The reactions typical of RPR1 (aldehydes) will be discussed in the next section. Oxidation or photolysis of RPR1 (reactions 300–302) leads to formation of RO₂20 or the corresponding acyl peroxy radical (RO₂55). The corresponding peroxy nitrate compound (PAN7), RO₂20, and 3-methyl-heptanoic acid (UR1) are formed in the reactions of RO₂55 (reactions 303-307). Details of acyl peroxy radical reactions will also be given in the next section. The reaction of OLEH with O₃ leads to the formation of HCHO, RPR1, ACID, UR1, CO, OH, HO₂, CO₂, ALKM (a reclassified reactive product), and RO₂20 in yields described in Table 2 and derived via Jenkin et al. [1997]. The OLEH-O(³P) reaction forms ALKM, RPR1, RO₂4, and RO₂20 in yields described in Table 2 and derived via *Atkinson* [1997].

3.3. Aldehydes

[18] Aldehydes, emitted in large amounts and formed via atmospheric chemistry, contribute significantly to the overall reactivity of the urban atmosphere [*Grosjean et al.*, 1996]. Degradation of formaldehyde (HCHO) occurs by photolysis (reactions 44 and 45) and oxidation by OH (reaction 46) and NO₃ (reaction 47). Higher *n*-aldehydes (ALD2) are represented by *n*-pentanal. Because of the importance of aldehyde reactions (with respect to RPR species leading to UR species capable of forming SOA), a

general aldehyde mechanism is discussed here. Like HCHO, higher aldehydes are degraded by OH, NO₃, or photolysis. OH and NO₃ degradation proceed via abstraction of the aldehydic H-atom and result in the formation of water or nitric acid and an acyl radical (RC(O)O₂·), after the subsequent addition of O₂. Photolysis is assumed to form a primary alkyl radical, CO, and an H-atom radical. The alkyl radical and the H-atom radical each react immediately with O₂ to form an alkyl peroxy radical and a hydroperoxy radical, respectively.

[19] The acyl peroxy radical can then undergo reaction with NO, NO₂, HO₂, and RO₂T. In the NO reaction, NO is converted to NO₂, resulting in decomposition of the remainder of the original radical to form CO₂ and a primary alkyl radical that immediately forms an alkyl peroxy radical upon addition of O₂. CO₂ and a primary alkyl peroxy radical are also formed in the RO₂T reaction. NO₂ adds to the radical to form a peroxy acyl nitrate species (denoted as PANi) that can thermally decompose back to RC(O)O₂· and NO₂. Acyl peroxy radicals are converted to organic acids in the reaction with HO₂. This pathway is less likely to occur relative to the NO or NO2 reactions under high NOx conditions typical of urban atmospheres [Niki et al., 1985; Moortgat et al., 1989] but accounts for one path of secondary formation of the organic acids observed in the atmosphere [Fraser et al., 1999; Nolte et al., 1999]. At present, the known routes of organic acid formation in the atmosphere cannot account for measured ambient concentrations [Jacob and Wofsy, 1988; Seinfeld and Pandis, 1998].

[20] The photolysis of ALD2 (reaction 59) leads to the formation of RO₂5, CO, and HO₂. Degradation of ALD2 by OH (reaction 60) and NO₃ (reaction 61) results in the corresponding acyl radical (RO₂6), which follows the chemistry described above (reactions 125 and 129). Products include NO₂, CO₂, RO₂5, ACID, O₃, and PAN1.

3.4. Ketones

- [21] Atmospheric ketones are less abundant than aldehydes [Fraser et al., 1997], but like aldehydes, they have both primary [Schauer, 1998; Schauer et al., 1999b] and secondary sources. Ketones in CACM are broken down into two groups: short chain ketones with between three and six carbons (KETL) and long chain ketones with seven or more carbons (KETH).
- [22] Ketones (for example, $R_1CH_2C(O)R_2$) either photolyze or are oxidized by OH [Atkinson, 1994]. It is assumed that the OH reaction proceeds via abstraction of the H-atom in the position α to the carbonyl functionality. After addition of O_2 , this results in the formation of $R_1CH(O_2 \cdot)C(O)R_2$, a ketoalkyl peroxy radical. Photolysis yields cleavage of the carbon-carbon bond adjacent to the carbonyl. After addition of O_2 , the results are $R_1CH_2O_2 \cdot$, a simple alkyl peroxy radical, and $R_2C(O)O_2 \cdot$, an acyl peroxy radical. The ketoalkyl peroxy radical, of course, reacts with NO, HO₂, and RO_2T to form an alkoxy radical in the position α to the carbonyl. This radical will decompose to form a higher aldehyde ($R_1C(O)H$) and the acyl peroxy radical described above.
- [23] KETL is represented by 2-pentanone because of the frequent occurrence of small chain ketones that have the functional group in the 2-position. Following the mecha-

nism described above, the reaction of KETL with OH (reaction 62) yields RO_27 , a keto-alkyl peroxy radical that is represented by a lumped structure with 4 carbons, the keto group in the 2-position, and the peroxy radical in the 3-position. Analogously, the photolysis of KETL (reaction 63) results in RO_25 and a 2-carbon acyl radical, RO_28 . Because RO_28 is formed in so many reactions in CACM, it is treated as a fully integrated species. RO_27 follows the reaction patterns (reactions 130-132) discussed earlier for alkyl peroxy radicals with carbonyls in the α -position. RO_28 follows the reaction patterns (reactions 133-137) discussed earlier for acyl peroxy radicals; the resulting products include peroxy acetyl nitrate (PAN2).

[24] Similarly, 2-heptanone represents KETH. Photolysis of KETH (reaction 71) also yields RO₂5 and RO₂8. Oxidation of KETH by OH (reaction 70) results in the formation of RO₂16, 2-keto-3-heptyl peroxy radical, which results in products identical to those of KETL (reactions 164–166). Because the final products formed by KETL and KETH are similar, separating them into two groups is based solely on kinetics.

3.5. Alcohols

- [25] Alcohols have both anthropogenic and biogenic sources [Harley et al., 1992; Goldan et al., 1993; Sharkey, 1996]. Hydroxyl groups, which characterize alcohols, are also present in multifunctional secondary organic oxidation products [Yu et al., 1999].
- [26] Methanol (MEOH) and ethanol (ETOH) have wellunderstood atmospheric chemistry [Atkinson, 1994]. Degradation of these compounds proceeds via OH abstraction of an H-atom from either a C-H or O-H bond. For MEOH (reaction 48), the resulting intermediates react instantaneously with O₂ to form HCHO and HO₂. For ETOH (reaction 53), the split between C-H and O-H abstraction is determined from the rate constants of each pathway [Kwok and Atkinson, 1995]. If the H-atom is abstracted from an O-H bond, the resulting intermediate immediately reacts with O₂ to form ALD2 and HO2. If the H-atom is abstracted from a C-H bond, the result is either ALD2 or RO₂2 depending on the location of the abstraction. Here 2-Hexanol represents alcohols with three or more carbon (ALCH). Abstraction by OH of an H-atom from the carbon chain is expected to be the dominant sink for ALCH (reaction 69). The resulting radical is RO₂2.

3.6. Methyl-Tert-Butyl Ether

[27] Because methyl-tert-butyl ether (MTBE) is a constituent of reformulated gasoline sold in the region during the period of interest, it is the only ether explicitly tracked in CACM. (Others are included in ALKL or ALKM as given by *Stockwell et al.* [1997].) Reaction of MTBE with OH (reaction 68) proceeds via H-atom abstraction and forms RO₂15. RO₂15 reacts with NO, HO₂, or RO₂T (reactions 161–163) to form ALD2, ALKL, KETL, and HCHO in yields described in Table 2 and based on the work of *Japar et al.* [1990] and the estimates of *Harley et al.* [1993].

3.7. Aromatics

[28] Aromatic species comprise a significant portion of the hydrocarbon component of motor vehicle emissions [Harley et al., 1992] and have been identified as the most

likely class of anthropogenic SOA precursors [*Odum et al.*, 1996, 1997]. Aromatics are found in relatively high concentrations in the urban atmosphere [*Fraser et al.*, 1999] and come from a variety of sources [*Schauer*, 1998; *Schauer et al.*, 1999a, 1999b].

[29] Aromatic species are aggregated depending on their reactivity, their degree and nature of substitution, and their potential for SOA formation, as determined by Odum et al. [1996, 1997]. Low SOA-yield aromatics (AROL, represented by 1,2,3-trimethylbenzene) are those with two or more methyl side groups and no functional side groups (such as phenols, aldehydes, acids, or nitro groups); high SOA-yield aromatics (AROH, represented by m-(n-propyl)toluene) have one or no methyl side groups and no functional side groups. Phenolic species (AROO, represented by 2,6-dimethyl-phenol) may have one or more alkyl side groups and one or more phenolic substituents. Aldehydic aromatics (ARAL, represented by p-tolualdehyde) have one aldehydic functional group; acidic aromatics (ARAC, represented by p-toluic acid) have one carboxylic functional group. Gas-phase polycyclic aromatic hydrocarbons (PAHs, represented by 1,2-dimethyl-naphthalene) have multiple aromatic rings. Generally, only PAHs with two aromatic rings remain in the gas-phase; those with more partition between the gas- and aerosol-phases [Fraser et al., 1999]. The chemistry of aromatics proceeds typically via OH addition to the ring or H-atom abstraction from alkyl side chains. Any deviations are explained appropriately in the sections below.

3.7.1. Low Yield Aromatics

[30] Products of AROL chemistry (reaction 79) include AROO, a cyclohexadienyl radical (RAD3), and RO221 (formed from H-atom abstraction from a side chain). The yields of these products are described in Table 2 and are derived from Atkinson [1990, 1994]. RO₂21 (reactions 179-181) forms a methyl nitrooxy substituted aromatic (AP4) or an aldehydic aromatic product (ARAL). AP4 is assumed to form ARAL as well (reaction 353). RAD3 can react either with NO₂ (reaction 105) to form nitro-trimethylbenzene (UR12) or predominantly with O₂ (reaction 98) to form a cyclohexadienyl peroxy radical (RO₂34), which can then isomerize (reaction 228) to form a bicyclic peroxy radical (RO₂43) or react with NO, HO₂, and RO₂T (reactions 229-231) [Klotz et al., 1997]. Reaction of RO₂34 leads to 4,5dimethyl-6-keto-2,4-heptadienal, RP11. RO₂43 reactions (232-234) form ring cleavage products such as methyl glyoxal (MGLY). The remaining unreactive ring cleavage products in this second pathway do not contribute to SOA formation so they are grouped together for all aromatic parents except PAH. They are represented by 2-methylbutenalic acid, RP10. In an effort to account for acid formation in aromatic oxidation (and the subsequent formation of SOA), RP11 reacts with OH (reaction 334) to form directly the corresponding acid (UR26) (as in the acyl radical reaction mechanism described in detail above), instead of undergoing the full range of aldehyde reactions. RP10 can either react with OH (reaction 332) to form the corresponding anhydride (UR24) or photolyze (reaction 333) to form the corresponding furan (UR25). MGLY is modeled to behave as an aldehyde, and follows the reaction pattern described earlier (reactions 263-365). Products of MGLY oxidation include RO₂8, CO, HO₂, and RO₂48, a 3-carbon,

keto-acyl radical. RO₂48 follows the acyl radical reaction pattern described above (reactions 266–270) and forms NO₂, CO₂, RO₂8, keto-peroxy-propionyl nitrate (PAN4), and keto-propanoic acid (UR21), which is considered capable of forming SOA because of its solubility in the aqueous phase. The chemistry of AROL is shown in Figure 1b.

3.7.2. High Yield Aromatics

[31] Because of the degree of substitution of this class of compounds, only ring addition is taken into account in the oxidation of AROH [Atkinson, 1994]. The products of this first step are AROO, HO₂, and a cyclohexadienyl (RAD4) radical similar to that formed in AROL oxidation. Yields are given in Table 2. Upon reaction with NO₂ (reaction 106), RAD4 forms the nitro-form of AROH (UR13). However, RAD4 predominantly reacts with O₂ (reaction 99) to form another cyclohexadienyl peroxy radical (RO₂35) that can isomerize (reaction 235) to form RO₂44 or react (reactions 236–238) to form primarily RP11. RO₂44 reacts (reactions 239–241) to form MGLY and RP10. The yield of the ring fragmentation products and kinetics are the only differences between the chemistry of AROL and AROH.

3.7.3. Phenolic Species

[32] In contrast to AROL and AROH, both NO₃ and OH can initiate oxidation of AROO. NO₃ abstracts the Hatom from the phenolic functional group (reaction 72) to form RAD1, a dimethyl-benzoxy radical. In an effort to account for observed concentrations of nitro-phenols [Fraser et al., 1999], it is assumed that RAD1 reacts only with NO₂ (reaction 103) to form dimethyl-nitro-phenol (RPR4). OH oxidation of AROO (reaction 73) proceeds via side chain abstraction (RO₂17) or addition to the ring to reform AROO or another cyclohexadienyl radical (RAD2). Yields for this reaction are presented in Table 2. RO₂17 reacts similarly to other organic peroxy radicals with the primary products including a nitrooxy derivative of AROO (AP1) and hydroxy-tolualdehyde (RPR2) (reactions 167-169). As before, RAD2 reacts predominantly with O₂ (reaction 97) to form a cyclohexadienyl peroxy radical (RO₂33) or can react with NO₂ (reaction 104) to form RPR4. RO₂33 can isomerize to RO₂42 (reaction 221) or can react (reactions 222-224) to form primarily 4hydroxy-3,5-dimethyl-2,4-hexadiendial, RPR9, RO₂42 (reactions 225-227) yields MGLY and RP10. Upon oxidation (reaction 350), AP1 will yield RPR2. Similarly to RP11, RPR2 reacts with OH (reaction 308) to form directly the corresponding acid (UR2). RPR9 also forms directly the corresponding acid (RP17) (reaction 331), which further reacts to form the corresponding diacid (UR29) (reaction 347).

3.7.4. Aromatic Aldehydes

[33] The degradation of ARAL by NO₃ (reaction 81) proceeds via abstraction of the aldehydic H-atom, resulting in the formation of HNO₃. In an effort to account for ambient concentrations of aromatic acids [Rogge et al., 1993; Fraser et al., 1999], it is assumed that the resulting acyl radical immediately reacts with HO₂ to form the corresponding aromatic acid (ARAC) and O₃. Degradation of ARAL by OH (reaction 82) can proceed via three distinct pathways: abstraction of the H-atom from the aldehyde group, abstraction of an H-atom from the methyl side group, or ring addition. The split between these is determined kinetically assuming that OH adds directly to the ring to

form a phenolic compound in the same yield as discussed previously. As with the NO₃ reaction, abstraction of the aldehydic H-atom leads directly to acid formation. Abstraction of an H-atom from the methyl group leads to the formation of RO₂22 which can proceed (reactions 182-184) to form primarily an aromatic compound with either one aldehyde and one nitrooxy-methyl side chain (AP5) or two substituent aldehyde side groups (RPR6). Upon oxidation (reaction 354), AP5 is converted to RPR6. Again in an effort to account for ambient formation of aromatic acids and diacids [Rogge et al., 1993; Fraser et al., 1999], the aldehyde groups of RPR6 are converted directly to acids (reactions 320 and 321). RPR7 describes an aromatic ring with one aldehyde and one acid substituent group. ADAC describes the aromatic species with two acid groups. (The URi notation is not used with ADAC, as aromatic diacids are also constituents of primary aerosol.) As with the other aromatic species discussed so far, addition of OH to the aromatic ring in ARAL results in the formation of a cyclohexadienyl radical, RAD5. As before, RAD5 can react with NO₂ (reaction 107) to form the corresponding nitro-tolualdehyde (RPR5) or with O₂ (reaction 100) to form the cyclohexadienyl peroxy radical, RO₂36. The aldehyde group of RPR5 can be converted directly to the acid (reaction 319) to form methyl-nitrobenzoic acid (UR14). Similar to the radicals formed from other aromatic species, RO₂36 can isomerize (reaction 242) to RO₂45 or undergo reaction (reactions 243–245) to form 2methyl-5-formyl-2,4-hexadiendial, RP12. RO₂45 reacts (reactions 246-248) to form MGLY and RP10. The three aldehyde groups of RP12 subsequently can be converted directly to acids forming, in order, RP13, RP18, and UR30 (reactions 335, 336, and 348).

3.7.5. Aromatic Acids

[34] Because the carboxylic acid moieties in CACM are considered unreactive, the degradation of ARAC is driven by reaction with OH (reaction 83) via either side chain Hatom extraction (RO₂23) or addition to the ring (UR2 or RAD6). Reactions of RO₂23 (reactions 185–187) yield either the methyl-nitrooxy derivative (AP6) or RPR7. When oxidized by OH (reaction 355), AP6 yields RPR7. Similar to other cyclohexadienyl radicals, RAD6 reacts predominantly with O₂ (reaction 101) to form the corresponding cyclohexadienyl peroxy radical (RO₂37) but can also react with NO₂ (reaction 108) to form the nitro derivative of ARAC (UR14). Isomerization of RO₂37 (reaction 249) leads to the formation of RO₂46, which reacts (reactions 253–255) to form RP10 and MGLY. Reaction of RO₂37 (reactions 250–252) leads to the formation of RP13.

3.7.6. Polycyclic Aromatic Hydrocarbons

[35] The final lumped aromatic compound considered in CACM is PAH. The sink for PAH is reaction with OH (reaction 92), which can lead to RO₂31 (H-atom abstraction from the side chain), UR11 (hydroxy-PAH), or an aromatic cyclohexadienyl radical (RAD7) similar to those formed by monoaromatic compounds. RO₂31 reacts (reactions 212–214) as before to form the methyl-nitrooxy derivative (AP10) and the aldehyde derivative (UR19). AP10 forms UR19 upon oxidation by OH (reaction 359). RAD7 reacts with O₂ (reaction 102) to form RO₂38 or with NO₂ (reaction 109) to form nitro-PAH (UR15). RO₂38 can isomerize (reaction 256) to RO₂47 or react (reactions 257–259) to form 2-(dimethyl propenal)-benzaldehyde (RP14). The

aldehyde groups in RP14 can be converted successively to acids, RP19 and UR31 (reactions 337 and 349). The reactions of RO₂47 (reactions 260–262) lead to MGLY and 2-formyl-acetophenone (RP15). The aldehyde group in RP15 can be converted to acid (reaction 338) resulting in the formation of 2-carboxy-acetophenone (UR27).

3.8. Biogenics

[36] Biogenic organics play an important role in atmospheric chemistry [Lamb et al., 1993; Guenther et al., 1995]. Isoprene (ISOP) and the monoterpenes are considered in CACM; sesquiterpenes are ignored because of their extremely low emission rate relative to those of isoprene and the monoterpenes and since little is known about their oxidation patterns.

3.8.1. Isoprene

[37] The atmospheric behavior of isoprene (ISOP), 2-methyl-1,3-butadiene, has been studied in detail [Paulson et al., 1992a, 1992b; Yu et al., 1995; Kwok et al., 1995; Carter and Atkinson, 1996]. ISOP does not contribute significantly to SOA formation [Pandis et al., 1991] but can contribute to ozone formation if emitted at a high enough rate. Because the mechanism of ISOP oxidation has been presented in detail previously, only an overview is given here.

[38] Like other unsaturated molecules, ISOP is oxidized by OH, NO₃, O₃, and O(3 P) (reactions 64–67). The mechanism in CACM assumes that OH and NO₃ addition to the double bonds occurs only at the two most probable spots, as determined by the stability of the resulting radicals [Atkinson, 1997]. The split between these locations is determined kinetically. The most preferred OH attack occurs first (approximately two thirds) in the 1-position and second (approximately one third) in the 4-position, resulting in a tertiary peroxy radical, RO₂9, and a secondary peroxy radical, RO₂10, respectively. The reactions of RO₂9 (reactions 138-140) are assumed to result in the formation of methyl-vinyl-ketone (MVK), HCHO, HO₂, and NO₂ (NO₂ in the NO case only). Correspondingly, the reactions of RO₂10 (reactions 141-143) result in the formation of methacrolein (MCR), HCHO, HO2, and NO2 (NO2 in the NO case only). The NO₃ oxidation pattern is analogous, with RO₂11 and RO₂12 having a nitrooxy group instead of an OH group. Upon reaction (reactions 144–149), these species liberate NO₂ and form MCR, MVK, HCHO, HO₂, and NO2. The ISOP-O3 reaction forms MVK, MCR, HCHO, OLEL (a reclassified small product), CO₂, ACID, CO, OH, HO₂, RO₂13, and RO₂14 in yields shown in Table 2 and derived from Jenkin et al. [1997]. RO₂13 is a 4carbon, unsaturated peroxy radical with a keto group and leads to HCHO and a 3-carbon, unsaturated acyl radical (RO₂39) (reactions 150-152). RO₂39 follows the previously discussed reaction pattern for acyl radicals (reactions 153-157) and results in the formation of RO₂14, CO₂, an unsaturated peroxy nitrate compound (PAN3), OLEL, ACID, and O₃. RO₂14 is a 2-carbon, unsaturated peroxy radical that is converted to OLEL or RO₂7 upon reaction (reactions 158–160). The ISOP-O(³P) reaction yields OLEL (reclassified) and ALD2 in yields shown in Table 2 and derived from Atkinson [1997].

[39] MCR and MVK are major oxidation products of ISOP and are included explicitly. MVK reacts with OH, O₃, and O(³P) (reactions 271–273); the NO₃ reaction is not consid-

ered because of its comparatively small rate constant (Carter/ SAPRC-99). OH reaction proceeds via addition and leads to the formation of RO₂49. Reactions of RO₂49 (274–276) lead to MGLY, HCHO, and HO₂ (and NO₂ in the NO reaction). The MVK-O₃ reaction results in the formation of MGLY, HCHO, ACID, UR21, ALD2, CO, CO₂, HO₂, OH, water, and RO₂8 in yields shown in Table 2 and derived from *Jenkin* et al. [1997]. Reaction between MVK and O(³P) leads to KETL (reclassified), RO₂4, and RO₂8 in yields shown in Table 2 and derived from Atkinson [1997]. MCR can also react with OH, NO₃, O₃, and O(³P) (reactions 277–280). The OH and NO₃ reactions can proceed via addition to the double bond (RO₂51 and RO₂52, respectively) or via H-atom abstraction from the aldehyde group (RO₂50). RO₂50 behaves similarly to the acyl radicals that have been described previously (reactions 281–285). Products include NO₂, CO₂, RO₂14, PAN5, ACID, and OLEL. RO₂51 and RO₂52 (reactions 286–291) lead to the formation of HCHO and MGLY. Reaction between MCR and O₃ leads to HCHO, MGLY, OH, CO, HO₂, ACID, and RO₂53 as shown in Table 2 with yields derived from Jenkin et al. [1997]. RO₂53 (reactions 292-294) leads to the formation of RO₂54, an aldehydic, 2-carbon acyl radical, which follows the reactions characteristic of acyl radicals (reactions 295-299). Products include NO2, CO2, CO, HO2, glyoxalic acid (RP16), and the corresponding peroxy nitrate compound (PAN6). Degradation of RP16 proceeds via photolysis (reaction 341) or abstraction of the aldehydic H-atom by OH or NO₃ (reactions 339 and 340). The abstraction pathway leads to the formation of the corresponding acyl radical (RO₂58) that will form products that include NO2, CO2, CO, OH, the corresponding peroxy nitrate species (PN10), and the corresponding acid (oxalic acid, UR28) (reactions 342–346). The chemistry of ISOP is illustrated in Figure 1c.

3.8.2. Monoterpenes

[40] Despite evidence that monoterpenes are not easily aggregated according to SOA formation potentials [Griffin et al., 1999], we lump them in this way because the uncertainties associated with monoterpene chemistry preclude representation at any greater level of detail. α-Terpineol, which represents relatively low SOA-yield monoterpenes (BIOL), encompasses the carbon number, structural characteristics, and reactivity of the group members as well. BIOL is oxidized by OH, NO₃, O₃, and O(³P) (reactions 84–87). OH addition to the double bond leads to RO₂24, a dihydroxy, tertiary peroxy radical. (NO₃ addition results in the analogous radical, RO225, with an ONO2 group replacing the OH group in the 2-position.) Reactions RO224 and RO₂25 (reactions 188–193) result in the nitrooxy product (AP7) and the keto-aldehyde (2-hydroxy-3-isopropyl-6keto-heptanal, RPR3) caused by ring cleavage. Upon oxidation (reaction 356), AP7 forms RPR3 as well. Oxidation of BIOL by O(³P) is assumed to result in two products (epoxide, UR5, and carbonyl, UR6) in yields estimated from Alvarado et al. [1998] and shown in Table 2. The attack by O₃ and resulting decomposition result in the formation of UR3, UR4, CO, RPR3, HO2, H2O2, OH, and RO226 in yields shown in Table 2 and derived from Jenkin et al. [1997]. UR3 and UR4 are the resulting hydroxy-keto-acid and keto-aldehyde, respectively. RO₂26 is a trisubstituted (hydroxy group, aldehyde, and ketone) organic peroxy radical. The reactions of RO₂26 (reactions 194–196) lead primarily to the formation of RO₂8 and UR17, a hydroxy dial. Reactions of RPR3 follow the reaction pattern assumed for aldehydes, as it assumed that the aldehyde is the most reactive moiety within RPR3. These reactions (reactions 309–311) result in the formation of the corresponding acyl radical (RO₂56) or UR4. The acyl radical reaction pattern followed by RO₂56 (reactions 312–316) leads to formation of NO₂, CO₂, UR4, PAN8, UR3, O₃, and UR4.

[41] CACM also incorporates a class (BIOH) for those monoterpenes that have relatively high SOA yield parameters [Griffin et al., 1999]. The structure chosen to represent this group is γ -terpinene because of its high reactivity and large SOA formation potential. As with all other unsaturated compounds, BIOH is oxidized by OH, NO₃, O₃, and O(³P) (reactions 88-91). OH addition is assumed to occur so that the peroxy radical is at the most stable possible location. The result is a cyclic, unsaturated, hydroxy peroxy radical (RO₂27). NO₃ oxidation occurs analogously to form the corresponding nitrooxy peroxy radical (RO₂28). Reactions of RO₂27 and RO₂28 (reactions 197-202) result in either the corresponding nitrooxy compound (AP8) or the ketoaldehyde ring cleavage product (UR7). UR7 is also formed by the reaction of AP8 with OH (reaction 357). In the $O(^{3}P)$ reaction, UR9 (epoxide) and UR10 (ketone) are formed in yields shown in Table 2 and derived from Alvarado et al. [1998]. The O₃-BIOH reaction leads to UR7, UR8, CO, OH, H₂O₂, RO₂29, and RO₂30 in yields shown in Table 2 and derived from Jenkin et al. [1997]. UR8 is the corresponding keto-acid ring cleavage product. RO₂29 is a primary peroxy radical with an unsaturated bond and a ketone moiety. Its reactions (203-205) lead to the appropriate nitrooxy product (AP9) or another peroxy radical (RO₂40) formed by isomerization. Upon oxidation (reaction 358), AP9 yields the corresponding unsaturated keto-aldehyde (UR33). The reactions of RO₂40 (206-208) lead to decomposition and the formation of RO₂8 and an unsaturated hydroxy aldehyde (RPR8). The corresponding reactions of RO₂30 (209-211), which exhibits an unsaturated bond, a ketone group, and an aldehyde, lead to the formation of UR18 (an unsaturated dial). Two photolysis pathways (reactions 324 and 325) are given for RPR8, one in which CO, HO₂, and RO₂9 are formed and another in which the corresponding acyl radical, RO₂57, is formed. (This is due to the α -position of the aldehyde relative to the unsaturated bond.) RO₂57 is also formed by the OH and NO₃ abstraction of the aldehydic H-atom from RPR8 (reactions 322 and 323, respectively). Following the behavior of other acyl radicals (in reactions 326-330), RO₂57 leads to RO₂9, CO₂, NO₂, the corresponding peroxy nitrate compound (PAN9), the corresponding acid (UR23), O₃, and RO_29 .

4. Gas-Phase Simulation of the SCAQS Episode of 27–29 August 1987 in the SoCAB

[42] We have presented a chemical mechanism for urban/regional atmospheric chemistry including SOA precursors. In its ozone formation chemistry, the mechanism builds upon previous work of *Stockwell et al.* [1997], *Jenkin et al.* [1997], Carter/SAPRC-97, and Carter/SAPRC-99. The mechanism is intended for use in three-dimensional urban/regional atmospheric models, where both ozone formation

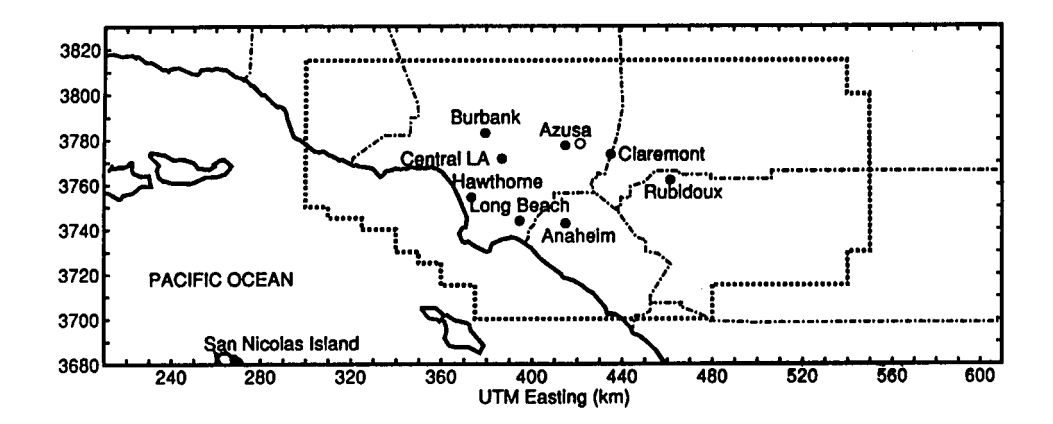


Figure 2. A map of the SoCAB. Major suburbs and downtown Los Angeles are indicated for reference.

and SOA production are to be predicted. As a prelude to these comprehensive simulations, it is of importance to establish the performance of the mechanism in ozone prediction. The SoCAB of California, because of the availability of both emissions inventories and comprehensive monitoring, has traditionally served as the benchmark for evaluating the performance of three-dimensional urban/ regional atmospheric models. Consequently, we present here a simulation of gas-phase chemistry in the SoCAB of California. We will evaluate ozone predictions of the new mechanism against both observed data and the earlier simulations of Harley et al. [1993]. The California Institute of Technology (CIT) model serves as the basic threedimensional model [Harley et al., 1993; Meng et al., 1998]; it conforms to the three-dimensional model structure embodied in the U.S. Environmental Protection Agency's Models 3 (available from the United States Environmental Protection Agency at http://www.epa.gov/ asmdnerl/models3/index.html), so modules presented in the present series of papers can be used in that framework as well.

4.1. The 27-29 August 1987 SCAQS Episode

[43] During the summer and fall of 1987, an intensive monitoring program known as the Southern California Air Quality Study (SCAQS) took place in the SoCAB [Lawson, 1990], which is shown graphically in Figure 2. The meteorological and air quality measurements made during this program provide a detailed ambient data set that has been used a number of times to evaluate atmospheric models. Previous simulations of the episode of 27-29 August 1987 include those of Harley et al. [1993], Harley and Cass [1995],

Table 7. Emissions Summary in 10³ kg/day Used in CIT for 27 August 1987

	NMHC	NO_x	СО
On-road vehicles	1229	678	4743
Other mobile sources	601	244	730
Ground-level point sources	379	123	139
Biogenic emissions	110	_	_
Other elevated point sources	6	60	8
Power plants	1	33	6
Total	2326	1138	5626

Jacobson et al. [1996], and Meng et al. [1998]. We will consider this episode as well to evaluate the performance of the gas-phase mechanism presented here. *Harley et al.* [1993] give emissions and boundary and initial conditions information for this episode. Therefore, only summary tables need be given here. Table 7 shows a highly aggregated emissions profile for one of the days simulated, and Table 8 gives the upwind boundary conditions. Harley et al. [1993] also describe the deposition module and meteorology used in CIT.

4.2. Ozone Simulation

[44] Predicted (dashed line) mixing ratios of O₃ (black) and NO (shaded) in Pasadena and Riverside are compared to data observed (solid line) at those locations in Figures 3 and 4, respectively. For Pasadena it is seen that O₃ is underpredicted on each day, with a slight shift in the peak predicted O₃ to a later time than that observed on the first day. NO simulations match observed data reasonably well except on the third day, when NO is significantly overpredicted at rush hour times (even though the third day is a Saturday). In Riverside, O₃ is underpredicted on the first day and matched well on the second and third days. Peak NO is underpredicted, but NO is slightly over predicted at night. These underpredictions and overpredictions are most likely linked to inaccuracies in the NO_x and gas-phase organic emissions inventories and uncertainties in the chemistry. These trends typify the predictions at other

Table & Unwind Boundary Condition Concentrations (nnh)

Table 6. Opwing Boundary Condition Concentrations (ppo)		
Species	Concentration	
CO	200	
NO_2	1	
NO	1	
НСНО	3	
ALD2	5	
KETL	4	
O_3	40	
NMHC (ppb C)	100	
Speciation ^a	Concentration	
ALKL	0.095	
ETHE	0.017	
OLEL	0.018	
AROH	0.015	
AROL	0.016	

^a Speciation in ppbv per ppb C of NMHC.

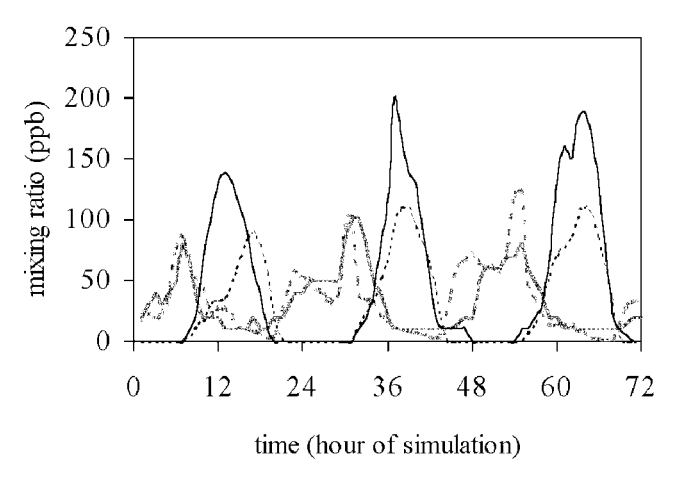


Figure 3. Simulated (dashed line) versus observed (solid line) NO (shaded) and O_3 (black) mixing ratios for Pasadena for 27-29 August 1987.

locations throughout the SoCAB. Pasadena and Riverside are chosen because they are downwind of major emissions sites and, thus, represent locations that are expected to display secondary species in higher concentrations.

[45] A statistical analysis of simulated results versus observed data has been performed for NO₂ and O₃ (Table 9). Statistics considered include bias, normalized bias, standard deviation, gross error, and normalized gross error. The methodology for these calculations is described by Harley et al. [1993]. These numbers are comparable to those of Harley et al. [1993] and, moreover, are typical of the level of agreement achieved in current three-dimensional modeling studies [Harley and Cass, 1995; Jacobson et al., 1996; Meng et al., 1998]. CACM predictions (dashed line) compared to those of Harley et al. [1993] (solid line) are shown for Pasadena and Riverside in Figures 5 and 6, respectively (using the same color scheme as Figures 3 and 4). In each case, O₃ CACM predictions usually exceed those from Harley et al. [1993]. Correspondingly, NO predictions are generally lower. Since the emissions, meteorology, and model structure are identical to those of Harley et al.

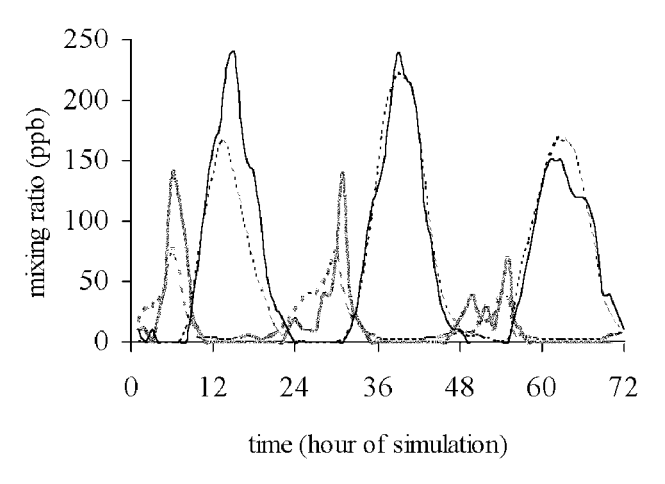


Figure 4. Simulated (dashed line) versus observed (solid line) NO (shaded) and O_3 (black) mixing ratios for Riverside for 27–29 August 1987.

Table 9. Statistical Analysis of CACM Performance on 28 August for O₃ and NO₂

Statistical Measure	O_3	NO_2
Bias, ppb	15.9	-0.4
Normalized bias, %	21.7	12.6
σ of residuals, ppb	55.3	28.1
Gross error, ppb	39.5	21.4
Normalized gross error, %	41.1	51.6

[1993], the differences seen in Figures 5 and 6 can be ascribed solely to changes in the chemical mechanism.

4.3. Total Semivolatile Species

[46] A principal goal of the gas-phase mechanism CACM is to predict concentrations of those surrogate organic products that have the potential to partition to the aerosol phase. Based on available or estimated vapor pressures or solubility, a product is considered to have the potential to partition to the aerosol phase if it meets one or more of the following criteria: (1) it is known to be partially soluble; (2) it is an aromatic acid; (3) it is an aromatic with two functional groups that are not aldehydes; (4) it has 12 or more carbon atoms (excluding primary gas-phase emission of ALKH and PAH); (5) it has at least 10 carbons and two functional groups; (6) it has at least six carbon atoms and two functional groups, one of which is an acid; or (7) it is trifunctional. The products considered capable of forming SOA based on these criteria are marked with a plus sign in Table 1. The total gas-phase concentration of those products represents the mechanism's prediction of the "atmospheric reservoir" of potential SOA components and is compared (solid line) in Figure 7 to observed concentrations of SOA (crosses) for 28 August 1987 in Claremont [Turpin and Huntzicker, 1995]. Figure 7 shows that the predicted temporal behavior of the total mass of compounds available to partition to SOA tracks well the pattern observed for ambient SOA. Figure 7 also shows that the mechanism predicts sufficient mass to account for the observed SOA concentrations.

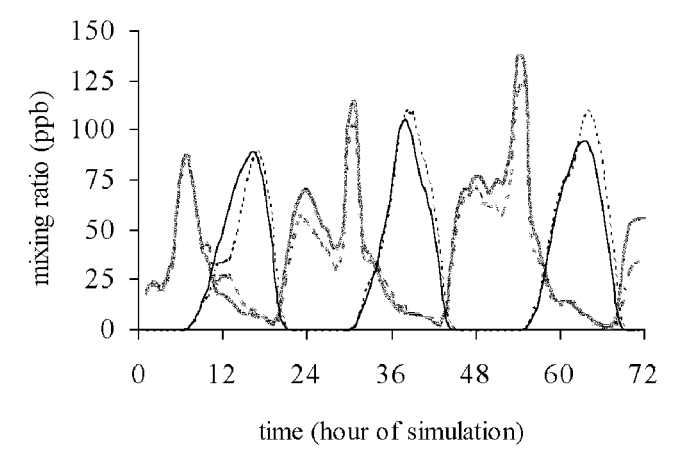


Figure 5. Mixing ratios simulated by CACM (dashed line) versus those simulated by the extended LCC mechanism (solid line) [*Harley et al.*, 1993] for Pasadena for 27-29 August 1987. NO is shown by shade line; O_3 is shown by black line.

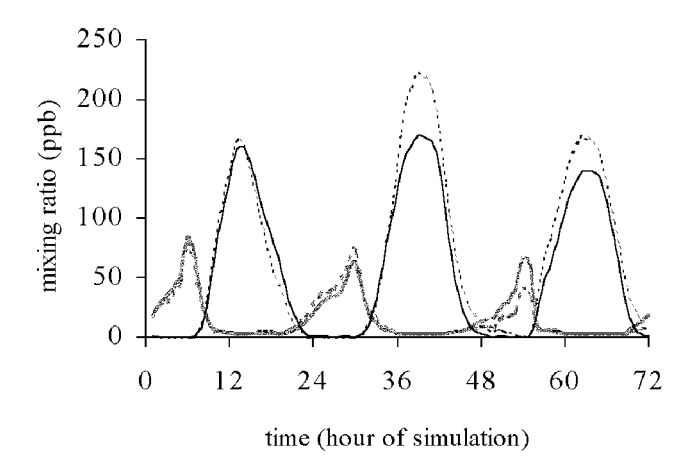


Figure 6. Mixing ratios simulated by CACM (dashed line) versus those simulated by the extended LCC mechanism (solid line) [*Harley et al.*, 1993] for Riverside for 27–29 August 1987. NO is shown by shaded line; O₃ is shown by black line.

[47] Reliable techniques for estimating/measuring ambient concentrations of SOA lag behind those for inorganic aerosol. The data of *Turpin and Huntzicker* [1995] presented here were generated by a technique that delineates primary organic carbon (OC) and elemental carbon (EC) aerosol concentrations under conditions when production of SOA should be low. The assumption made with this technique is that EC and primary OC have the same sources, so that a representative ratio of primary OC to EC for a

given region exists. In order to determine this ratio, ambient measurements of the OC/EC ratio are made on days when photochemical activity is expected to be low or an average ratio is obtained by determining the ratio at individual emissions sites. Subsequent ambient measurements are then made during times when photochemical activity is expected to occur, and it is assumed that if the ambient value of OC/ EC is greater than the characteristic primary OC/EC value, the excess OC consists of SOA [Turpin and Huntzicker, 1995]. The main advantage of this approach is its simplicity; however, there are associated uncertainties. First, the primary OC/EC ratio varies from source to source and may be dependent on factors such as meteorology, time of day, and season. Also, obtaining an average primary OC/EC ratio is difficult because of problems associated with sampling of semivolatile organics, and it has been shown that different sample collection and analysis techniques result in different values for this ratio at the same location and time [McMurry, 1989; Turpin and Huntzicker, 1995]. Finally, even on days when there is little potential for photochemical activity, previously formed SOA may be present from prior days.

4.4. Uncertainty Analysis

[48] Historically, among all the uncertainties associated with three-dimensional urban/regional atmospheric simulations, the largest are those associated with the emissions inventory. From a chemical mechanism perspective, uncertainty lies in the rate constants, the product yields, and the mechanisms of degradation of second, third, and further generation products. These issues have been discussed in

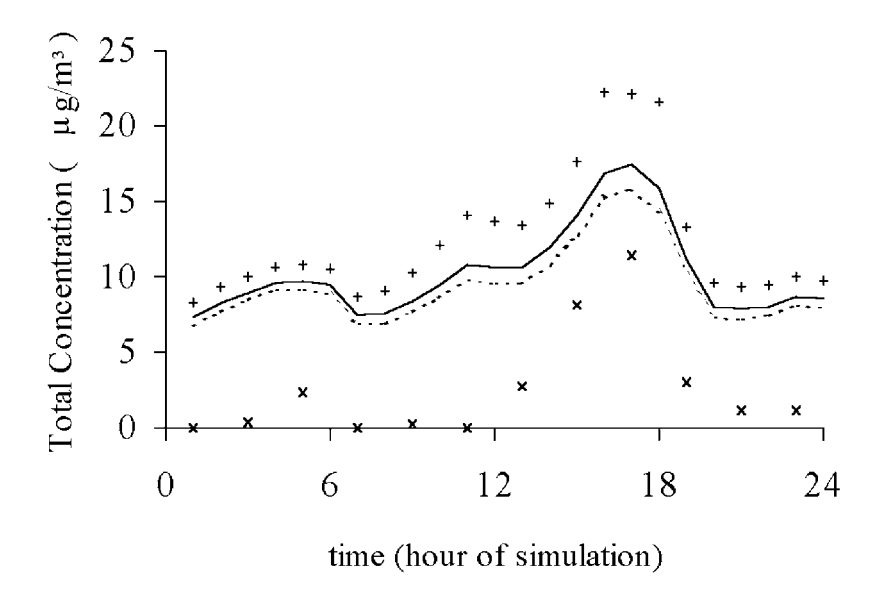


Figure 7. Comparison of total predicted SOA precursor concentration in the base case (solid line) versus observed SOA data (crosses) in Claremont on 28 August 1987. The data of *Turpin and Huntzicker* [1995] were converted from $\mu g C/m^3$ to $\mu g/m^3$ by multiplying by a factor of 1.2 [Countess et al., 1980]. Also shown is the sensitivity of the total predicted SOA precursor concentrations to the aromatic radical isomerization rate constant and to the yield of direct conversion of certain aldehydes to acids. The b/2 (pluses) represents the case in which the base case aromatic radical isomerization rate constant is divided by 2; acid (dashed line) represents the case in which the yield of direct conversion of certain aldehydes to acids is divided by 2.

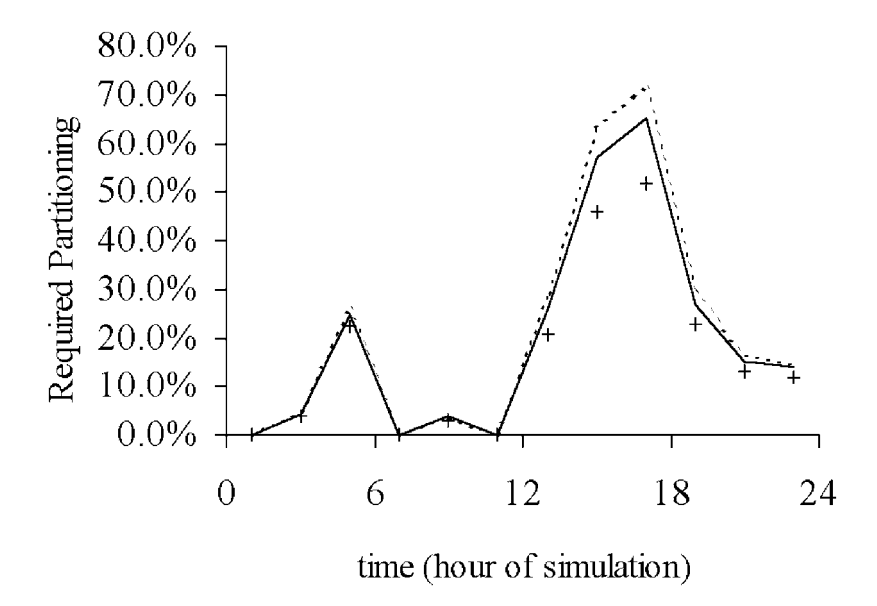


Figure 8. Percentage of the total SOA precursor concentration that must partition to account for the observations of *Turpin and Huntzicker* [1995] for the three cases investigated. Solid line represents the base case, plus sign represents the b/2 case, and dashed line represents the acid case.

detail previously [Harley et al., 1993; Jacobson et al., 1996; Stockwell et al., 1997]. While there are a number of areas of uncertainty in the chemical mechanism that one might select for analysis, space does not permit a lengthy analysis of such uncertainties, especially with regard to ozone formation. However, it is informative in the present case to investigate aspects of the chemical mechanism to which prediction of semivolatile products might be especially sensitive.

[49] Because aromatics are known to be an important source of anthropogenic SOA [Odum et al., 1996] and because uncertainties in aromatic chemistry have been well documented [Atkinson, 1994], an issue that merits evaluation here is the sensitivity of SOA predicted from aromatic precursors to key aspects of aromatic photooxidation. One particular rate constant that has the potential to be especially influential is that which describes the isomerization of radicals formed in aromatic-OH chemistry (reactions 221, 228, 235, 242, 249, and 256) [Lay et al., 1996]. This rate constant affects SOA formation because slower isomerization will lead to less MGLY and RP10 formation and more formation of semivolatile products. Because earlier models generally underpredicted organic aerosol [Meng et al., 1997, 1998], we consider here only the effect of halving the isomerization rate constant in an uncertainty analysis. Changes between the two cases are very small for NO, NO_2 , and O_3 ; there is a slight decrease in O_3 , a slight increase in NO, and mixed results for NO2. Figure 7 also compares the total amount of organic material available to partition to SOA in Claremont on 28 August 1987 in the base case (solid line) and that in which the bridging rate constant is halved (b/2 case, plus signs). It is seen that decreasing the bridging rate constant results in a significant increase in the amount of organic mass with the potential to form SOA, especially in the early morning and early afternoon.

[50] A second source of uncertainty in the chemical mechanism is the direct conversion of aldehydes to acid groups in certain reactive products. Although the exact mechanism of this conversion remains elusive, such a step attempts to account for observed ambient concentrations of semivolatile organic acids [Rogge et al., 1993; Nolte et al., 1999]. Since assuming 100% conversion certainly overestimates acid formation, this yield is also halved (reactions 81, 82, 308, 319, 320, 321, 331, 334, 335, 336, 337, 338, 347, 348, and 349). Figure 7 also shows the results for this scenario (acid case, dashed line) for 28 August 1987 in Claremont. While there are essentially no changes in the simulations for O₃ and NO_x in this case, predictions of total SOA material are seen to decrease as expected. However, the magnitude of these changes is not as large as that of the b/2 case (plus signs). Figure 8 shows the percentage of the total SOA precursor concentration that must partition to account for the observations of Turpin and Huntzicker [1995] in the base case (solid line), the b/2 case (plus signs), and the acid case (dashed line). It is seen that in each case, sufficient concentrations of SOA precursor material are predicted to account for the observations of Turpin and Huntzicker [1995].

5. Conclusions

[51] Previous gas-phase mechanisms describing urban/regional atmospheric chemistry have focused primarily on describing the formation of ozone. This paper describes a new chemical mechanism, the Caltech Atmospheric Chemistry Mechanism (CACM), that describes explicitly organic chemistry in an effort to predict the concentrations of secondary and tertiary organic oxidation products that can act as constituents of secondary organic aerosol. Parent organics in CACM must be aggregated into lumped surrogate structures. In total, CACM includes 191 species: 120

fully integrated species (15 inorganic, 71 reactive organic, and 34 unreactive organic), 67 pseudo-steady-state species (2 inorganic and 65 organic), and 4 species that have fixed concentrations. These species participate in over 360 reactions.

[52] CACM has been used in the three-dimensional CIT model to predict gas-phase concentrations in the South Coast Air Basin of California for 27-29 August 1987. As part of the Southern California Air Quality Study, ambient measurements were taken during these dates, providing data to which the model results can be compared. As shown in this paper, the predicted mixing ratios of O₃, NO, and NO₂ are statistically comparable to those predicted by the extended mechanism of Lurmann et al. [1987], which has been used in the CIT model previously [Harley et al., 1993]. Concentrations of secondary and tertiary organic oxidation products capable of forming secondary organic aerosol will be passed to a model designed to predict equilibrium gas-aerosol partitioning of organic oxidation products (part 2). The development of CACM is a first step in allowing for more rigorous treatment of secondary organic aerosol formation in atmospheric models than has been possible previously.

[53] **Acknowledgments.** This work was funded by the United States Environmental Protection Agency under grant R826371-01, by the State of California Air Resources Board under contract 98-314, and by the Electric Power Research Institute. Although the research described in this article has been funded in part by the U. S. Environmental Protection Agency's STAR program through grant R826371-01, it has not been subjected to any EPA review and therefore does not necessarily reflect the views of the Agency, and no official endorsement should be inferred.

References

- Alvarado, A., E. C. Tuazon, S. M. Aschmann, R. Atkinson, and J. Arey, Products of the gas-phase reactions of O(³P) atoms and O₃ with α-pinene and 1,2-dimethyl-1-cyclohexene, *J. Geophys. Res.*, 103, 25,541–25,552, 1098
- Atkinson, R., Gas-phase tropospheric chemistry of organic compounds: A review, Atmos. Environ., Part A, 24, 1–41, 1990.
- Atkinson, R., Gas-phase tropospheric chemistry of organic compounds, J. Phys. Chem. Ref. Data, 2, 1994.
- Atkinson, R., Gas-phase tropospheric chemistry of volatile organic compounds, 1, Alkanes and alkenes, J. Phys. Chem. Ref. Data, 26, 215–290, 1997.
- Barthelmie, R. J., and S. C. Pryor, A model mechanism to describe oxidation of monoterpenes leading to secondary organic aerosol, *J. Geophys. Res.*, 104, 23,657–23,669, 1999.
- Carter, W. P. L., and R. Atkinson, Alkyl nitrate formation from the atmospheric photooxidation of alkanes: A revised estimation method, *J. Atmos. Chem.*, 8, 165–173, 1989.
- Carter, W. P. L., and R. Atkinson, Development and evaluation of a detailed mechanism for the atmospheric reactions of isoprene and NO_x, *Int. J. Chem. Kinet.*, 28, 497–530, 1996.
- Countess, R. J., G. T. Wolff, and S. H. Cadle, The Denver winter aerosol: A comprehensive chemical characterization, *J. Air Pollut. Control Assoc.*, 30, 1194–1200, 1980.
- Dransfield, T. J., K. K. Perkins, N. M. Donahue, J. G. Anderson, M. M. Sprengnether, and K. L. Demerjian, Temperature and pressure dependent kinetics of the gas-phase reaction of the hydroxyl radical with nitrogen dioxide, *Geophys. Res. Lett.*, 26, 687–690, 1999.
- Fraser, M. P., G. R. Cass, B. R. T. Simoneit, and R. A. Rasmussen, Air quality model evaluation data for organics, 4, C₂-C₃₆ aromatic hydrocarbons, *Environ. Sci. Technol.*, 31, 2356–2367, 1997.
- Fraser, M. P., G. R. Cass, and B. R. T. Simoneit, Particulate organic compounds emitted from motor vehicle exhaust and in the urban atmosphere, Atmos. Environ., 33, 2715–2724, 1999.
- Gery, M. W., G. Z. Whitten, J. P. Killus, and M. C. Dodge, A photochemical mechanism for urban and regional scale computer modeling, J. Geophys. Res., 94, 12,925–12,956, 1989.
- Goldan, P. D., W. C. Kuster, F. C. Fehsenfeld, and S. A. Montzka, The

- observation of a C_5 alcohol emission in a North American pine forest, *Geophys. Res. Lett.*, 20, 1039–1042, 1993.
- Goumri, A., L. Elmaimouni, J.-P. Sawyersyn, and P. Devolder, Reaction rates at (297 +/-3)K of four benzyl-type radicals with O₂, NO, and NO₂ by discharge flow/laser induced fluorescence, *J. Phys. Chem.*, *96*, 5395–5400, 1992.
- Griffin, R. J., D. R. Cocker III, R. C. Flagan, and J. H. Seinfeld, Organic aerosol formation from the oxidation of biogenic hydrocarbons, *J. Geo*phys. Res., 104, 3555–3567, 1999.
- Grosjean, E., D. Grosjean, M. P. Fraser, and G. R. Cass, Air quality model evaluation data for organics, 2, C₁-C₁₄ carbonyls in Los Angeles, *Envir*on. Sci. Technol., 30, 2687–2703, 1996.
- Guenther, A., et al., A global model of natural volatile organic compound emissions, *J. Geophys. Res.*, 100, 8873–8892, 1995.
- Harley, R. A., and G. R. Cass, Modeling the atmospheric concentrations of individual volatile organic compounds, *Atmos. Environ.*, 29, 905–922, 1995
- Harley, R. A., M. P. Hannigan, and G. R. Cass, Respeciation of organic gas emissions and the detection of excess unburned gasoline in the atmosphere, *Environ. Sci. Technol.*, 26, 2395–2408, 1992.
- Harley, R. A., A. G. Russell, G. J. McRae, G. R. Cass, and J. H. Seinfeld, Photochemical modeling of the Southern California Air Quality Study, Environ. Sci. Technol., 27, 378–388, 1993.
- Hoffmann, T., J. R. Odum, F. Bowman, D. Collins, D. Klockow, R. C. Flagan, and J. H. Seinfeld, Formation of organic aerosols from the oxidation of biogenic hydrocarbons, *J. Atmos. Chem.*, 26, 189–222, 1997.
- Jacob, D. J., and S. C. Wofsy, Photochemistry of biogenic emissions over the Amazon forest, J. Geophys. Res., 93, 1477-1486, 1988.
- Jacobson, M. Z., R. Lu, R. P. Turco, and O. B. Toon, Development and application of a new air pollution modeling system, 1, Gas-phase simulations, *Atmos. Environ.*, 30, 1939–1963, 1996.
- Japar, S. M., T. J. Wallington, J. F. O. Richert, and J. C. Ball, The atmospheric chemistry of oxygenated fuel additives: Tert-butyl alcohol, dimethyl ether, and methyl-tert-butyl ether, *Int. J. Chem. Kinet.*, 22, 1257–1269, 1990.
- Jenkin, M. E., S. M. Saunders, and M. J. Pilling, The tropospheric degradation of volatile organic compounds: A protocol for mechanism development, *Atmos. Environ.*, 31, 81–104, 1997.
- Klotz, B., I. Barnes, K. H. Becker, and B. T. Golding, Atmospheric chemistry of benzene oxide/oxepin, *J. Chem. Soc. Faraday Trans.*, 93, 1507–1516, 1997.
- Kwok, E. S. C., and R. Atkinson, Estimation of hydroxyl radical reaction rate constants for gas-phase organic compounds using a structure-reactivity relationship: An update, *Atmos. Environ.*, 29, 1685–1695, 1995.
- Kwok, E. S. C., S. M. Aschmann, J. Arey, and R. Atkinson, Product formation from the reaction of the NO₃ radical with isoprene and rate constants for the reactions of methacrolein and methyl vinyl ketone with the NO₃ radical, *Int. J. Chem. Kinet.*, 28, 925–934, 1995.
- Lamb, B., D. Gay, H. Westberg, and T. Pierce, A biogenic hydrocarbon emission inventory for the U.S.A. using a simple forest canopy model, *Atmos. Environ.*, 27, 1673–1690, 1993.
- Lawson, D. R., The Southern California Air Quality Study, J. Air Waste Manage. Assoc., 40, 156–165, 1990.
- Lay, T. H., J. W. Bozzelli, and J. H. Seinfeld, Atmospheric photochemical oxidation of benzene: Benzene + OH and the benzene-OH adduct (hydroxyl-2,4-cyclohexadienyl) + O₂, J. Phys. Chem., 100, 6543-6554, 1996
- Lurmann, F. W., W. P. L. Carter, and L. A. Coyner, A surrogate species chemical reaction mechanism for urban-scale air quality simulation models, EPA Rep. 600/3-87/014A, Environ. Prot. Agency, Washington, D. C., 1987.
- McMurry, P. H., Final report to the California Air Resources Board under contract A732-075, report, Calif. Air Res. Board, Sacramento, Calif., 1080
- McRae, G. J., Mathematical modeling of photochemical air pollution, Ph.D. thesis, Calif. Inst. of Technol., Pasadena, 1981.
- Meng, Z., D. Dabdub, and J. H. Seinfeld, Chemical coupling between atmospheric ozone and particulate matter, Science, 277, 116–119, 1997.
- Meng, Z., D. Dabdub, and J. H. Seinfeld, Size-resolved and chemically resolved model of atmospheric aerosol dynamics, J. Geophys. Res., 103, 3419–3435, 1998.
- Moortgat, G. K., B. Veyret, and R. Lesclaux, Kinetics of the reaction of HO₂ with CH₃C(O)O₂ in the temperature range 253–368K, *Chem. Phys. Lett.*, 160, 443–447, 1989.
- Niki, H., P. D. Maker, C. M. Savage, and L. P. Breitenbach, FTIR study of the kinetics and mechanism of Cl-atom-initiated reactions of acetaldehyde, J. Phys. Chem., 89, 588–591, 1985.
- Nolte, C. G., M. P. Fraser, and G. R. Cass, Gas-phase C₂-C₁₀ organic acid concentrations in the Los Angeles atmosphere, *Environ. Sci. Technol.*, 33, 540–545, 1999.

- Odum, J. R., T. Hoffmann, F. Bowman, D. Collins, R. C. Flagan, and J. H. Seinfeld, Gas/particle partitioning and secondary organic aerosol yields, *Environ. Sci. Technol.*, 30, 2580–2585, 1996.
- Odum, J. R., T. P. W. Jungkamp, R. J. Griffin, R. C. Flagan, and J. H. Seinfeld, The atmospheric aerosol-forming potential of whole gasoline vapor, *Science*, 276, 96–99, 1997.
- Pandis, S. N., S. E. Paulson, J. H. Seinfeld, and R. C. Flagan, Aerosol formation in the photooxidation of isoprene and β-pinene, *Atmos. Envir*on., 25, 997–1008, 1991.
- Pankow, J. F., J. H. Seinfeld, W. E. Asher, and G. B. Erdakos, Modeling the formation of secondary organic aerosol, 1, The application of theoretical principles to measurements obtained in the α-pinene-, β-pinene-, sabinene-, Δ^3 -carene-, and cyclohexene-ozone systems, *Environ. Sci. Technol.*, 35, 1164–1172, 2001.
- Paulson, S. E., R. C. Flagan, and J. H. Seinfeld, Atmospheric photooxidation of isoprene, 1, The hydroxyl radical and ground-state atomic oxygen reactions, *Int. J. Chem. Kinet.*, 24, 79–101, 1992a.
- Paulson, S. E., R. C. Flagan, and J. H. Seinfeld, Atmospheric photooxidation of isoprene, 2, The ozone-isoprene reaction, *Int. J. Chem. Kinet.*, 24, 103–125, 1992b.
- Rogge, W. F., M. A. Mazurek, L. M. Hildemann, G. R. Cass, and B. R. T. Simoneit, Quantification of urban organic aerosols at a molecular-level-identification, abundance and seasonal-variation, *Atmos. Environ., Part A*, 27, 1309–1330, 1993.
- Schauer, J. J., Source contributions to atmospheric organic compound concentrations: Emissions, measurements, and model predictions, Ph.D. thesis, Calif. Inst. of Technol., Pasadena, 1998.
- Schauer, J. J., M. J. Kleeman, G. R. Cass, and B. R. T. Simoneit, Measurement of emissions from air pollution sources, 1, C₁ through C₂₉ organic compounds from meat charbroiling, *Environ. Sci. Technol.*, 33, 1566–1577, 1999a.
- Schauer, J. J., M. J. Kleeman, G. R. Cass, and B. R. T. Simoneit, Measurement of emissions from air pollution sources, 2, C₁ through C₃₀ organic compounds from medium duty diesel trucks, *Environ. Sci. Technol.*, 33, 1578–1587, 1999b.

- Seinfeld, J. H., and S. N. Pandis, Atmospheric Chemistry and Physics, Wiley-Interscience, New York, 1998.
- Sharkey, T. D., Emission of low-molecular mass hydrocarbons from plants, *Trends Plant Sci.*, 1, 78–82, 1996.
- Stockwell, W. R., P. Middleton, J. S. Chang, and X. Tang, The second generation Regional Acid Deposition Model chemical mechanism for regional air quality modeling, *J. Geophys. Res.*, 95, 16,343–16,367, 1990.
- Stockwell, W. R., F. Kirchner, M. Kuhn, and S. Seefeld, A new mechanism for regional atmospheric chemistry modeling, *J. Geophys. Res.*, 102, 25,847–25,879, 1997.
- Turpin, B. J., and J. J. Huntzicker, Identification of secondary organic aerosol episodes and quantitation of primary and secondary organic aerosol concentrations during SCAQS, Atmos. Environ., 29, 3527–3544, 1995.
- Yu, J., H. E. Jeffries, and R. M. LeLacheur, Identifying airborne carbonyl-compounds in isoprene atmospheric photooxidation products by their PFBHA oximes using gas-chromatography ion-trap mass spectrometry, *Environ. Sci. Technol.*, 29, 1923–1932, 1995.
- Yu, J., D. R. Cocker III, R. J. Griffin, R. C. Flagan, and J. H. Seinfeld, Gasphase ozone oxidation of monoterpenes: Gaseous and particulate products, J. Atmos. Chem., 34, 207–258, 1999.
- D. Dabdub, Department of Mechanical and Aerospace Engineering, University of California at Irvine, Irvine, CA 92697-3975, USA. (ddabdub@uci.edu)
- R. J. Griffin, Department of Civil and Environmental Engineering, Duke University, Box 90287, Durham, NC 27708-0287, USA. (robgriff@duke.edu)
- J. H. Seinfeld, Department of Chemical Engineering and Division of Engineering and Applied Science, California Institute of Technology, Mail Code 210-41,1200 East California Boulevard, Pasadena, CA 91125, USA. (seinfeld@caltech.edu)